ABSTRACT

PINER, EMILY VALLERY. Fully Bio-Based Barrier Films and Coatings for Use in the Packaging Industry: Understanding the Interactions Between Composite Components. (Under the direction of Dr. Nathalie Lavoine and Dr. Lucian A. Lucia).

The accumulation of solid plastic waste in the environment is one of many environmental concerns in the public conscious today. Plastic packaging is the single biggest contributor to this waste. Biopolymers offer a potential solution in that they are abundant, sustainable, and potentially biodegradable. Of particular note are cellulose and lignin as they have many unique properties that could be leveraged into a packaging application. This work aims to develop use combinations of different biopolymers to develop fully bio-based sustainable alternatives to petroleum-based packaging films and coatings.

This work is divided into two main sections the first of which is the development of bacterial nanocellulose composite films. Bacterial nanocellulose has many properties that are of use in the food packaging industry including high oxygen barrier and mechanical strength. However, the water sensitivity of the cellulose must be circumvented for it to be a practical material for use as food packaging. Thin, translucent, and flexible films of bacterial nanocellulose, alginate, and zein were formed by solvent casting of an alkaline aqueous suspension containing different weight ratios of each material. Alginate was chosen to enhance the mechanical properties of the films, especially in wet state, as well as its unique ability to be crosslinked with divalent metal cations. Zein was chosen because it is an amphiphilic protein and was potentially able to increase the water barrier properties of the resulting films. The study of bi-component films of bacterial nanocellulose and either alginate or zein showed that the addition of 10 w% of the alginate zein to the bacterial nanocellulose suspension improved the film performance. Further

improvement of the overall performance of the composite films, and in particular, a 100% increase in the elongation at break was obtained by crosslinking of alginate using calcium chloride.

These results allowed for the creation of three component films with 80 w% bacterial nanocellulose, 10 w% alginate, and 10 w% zein that showed a synergistic action by increasing the water contact angle to 75°, while increasing the water vapor permeability and water absorption as well. A conceptual model of the arrangement of the three biopolymers within the films was developed with the aid of SEM and XPS to explain the mechanical and water barrier performance of the films. In this model, the bacterial nanocellulose and alginate form an interpenetrating network and the zein adheres to the surface of the bacterial nanocellulose via ion-dipole interactions between the polar groups at the surface of the cellulose and the carboxylate ions on the zein. Crosslinking of the system with calcium chloride alters the model with the formation of ionic bonds between the alginate and the calcium ions, and between the calcium ions and the carboxylate ions on the zein, resulting in spherical zein aggregates throughout the film structure.

The second section of this thesis is the development of a lignin-based coating for moisture barrier applications. A bio-based coating was formulated by chemically bonding kraft lignin to epoxidized soy lecithin via a combination of ester and sulfide bonds. The water vapor permeability was assessed at different solids contents as well as with the addition of a plasticizer. The application of this coating to a porous, rough cellulosic surface such as one side coated paperboard greatly reduced its water vapor permeability by 57%, but when applied to a non-porous, flat surface such as a commercial plastic film, such a reduction was not observed. These results show that the lignin-based coating has potential as a water barrier layer in multilayer packaging for enhanced sustainability. Further optimization is still required to advance the commercialization of the proposed solution as the water vapor permeability is 19% higher than that of the uncoated films.

Fully Bio-Based Barrier Films and Coatings for Use in the Food Packaging Industry: Understanding the Interactions Between Composite Components

by
Emily Vallery Piner

A thesis submitted to the Graduate Faculty of
North Carolina State University
in partial fulfillment of the
requirements for the degree of
Master of Science

Forest Biomaterials

Raleigh, North Carolina

2022

APPROVED BY:

_____	_____
Dr. Nathalie Lavoine	Dr. Lucian A. Lucia
Committee Co-Chair	Committee Co-Chair

_____
Dr. Saad Khan

DEDICATION

To Will who inspired me to start and forced me to finish this endeavor.

BIOGRAPHY

Emily Piner received a B.S. in Chemistry with a minor in Spanish from the University of North Carolina – Wilmington in 2014. While there, she participated in undergraduate research on the organic synthesis of small, bio-active molecules for potential use as anti-inflammatory agents.

After graduation, Emily taught high school science within the New York City Department of Education, Craven County Schools, and Wake County Public School System. While working at Green Hope High School she became involved in the Sustainable Bioproducts and Bioenergy Program within the Department of Forest Biomaterials at North Carolina State University. She found the research being done within the department inspiring and decided to leave teaching and return to graduate school.

As a masters student, Emily has worked on several projects all focused on making barrier films and coatings from biomaterials. While completing her research and coursework she also found time to contribute to the overall department and campus community. She was a member of the Forest Biomaterials Analytical Team and oversees the maintenance of and training of users for both the TGA and UV/VIS equipment. Additionally, she volunteered at the Feed the Pack food pantry on a weekly basis.

After completing her masters, she will spend the summer as an intern with the US Environmental Protection Agency before pursuing her PhD in chemistry at NCSU in the fall.

ACKNOWLEDGMENTS

The number of people deserving of acknowledgement is far too great to list. Instead, I will say that the trajectory of my life has changed from my experiences here in the Department of Forest Biomaterials and that each person with whom I interacted contributed to that. I sincerely thank each and every one of you for being in my life.

TABLE OF CONTENTS

LIST OF TABLES

LIST OF FIGURES

CHAPTER 1: Introduction

1.1 Motivation

Plastic pollution is among the most visible issues facing our environment. Mitigating the amount of plastic waste that enters our terrestrial, freshwater, and marine ecosystems has been a major talking point at the global level for more than a decade[1,2]. Many companies have responded to this pressure with sustainability initiatives[3], and recently more than 180 countries agreed to ban the international trade of plastic waste in an attempt to stem the tide of plastic pollution[4]. In a 2021 report, the United Nations found that the COVID-19 pandemic exacerbated this issue by driving demand for disposable plastics up and the prices for plastic resins down. Furthermore, the impact of plastic waste disproportionately effects low-income and marginalized communities[5]. The need for an answer to these challenging issues becomes more obvious with each passing year.

Plastic is a ubiquitous part of modern life with global production increasing from 2 million metric tons in 1950 to over 380 million metric tons in 2015[6]. As production has increased, the ultimate fate of the plastic waste has also changed. Before 1980 all plastics were discarded after use but as recycling technology has developed that number has decreased to between 55 and 75% depending on the location and type of plastic waste generated[6,7]. The packaging industry is the largest contributor of plastic waste, producing approximately 141 million metric tons (47%) of plastic waste in 2015 **(Fig. 1.1)**. These values include all solid plastic waste including coatings and sealants from the most commonly used, petroleum-derived, resins (e.g. polyethylene, polypropylene, polystyrene, polyvinylchloride, polyethylene terephthalate, and polyurethane as well as polyester, polyamide and acrylic fibers). The large amount of waste generated is due in part to the single-use nature of most plastic packaging products. As such, there exists a need for

sustainable plastic alternatives that can be used as packaging that does not persist in the environment.

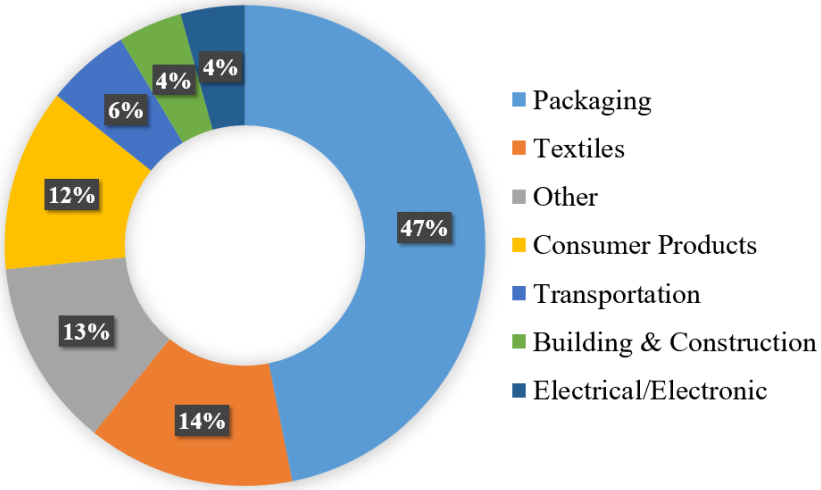

Figure 1.1. Plastic waste generated by market sector in 2015. (Adapted from Geyer et al., 2017.)

1.2 The Unique Challenges of Plastic Packaging

The high-performance nature of many plastic packaging materials presents an interesting sustainability challenge. Depending on the intended use, packaging plastic may need varying levels of strength, flexibility, and permeability, among others[8]. For example, soft drink bottles are frequently made of polyethylene terephthalate (PET) which is clear, lightweight, and strong enough to withstand the pressure of the carbonated beverage. However, PET is susceptible to heat degradation and has a glass transition temperature of approximately 70 °C; therefore it cannot be used in hot applications like coffee cups or cookware[9]. This wide variety of applications for plastic materials implies that there may not be a single solution to match the performance of all plastics.

Plastic films are frequently used as standalone packaging like Saran Wrap, but are also often combined with other plastic films, metals, and paper to create multilayer packaging substrates with greater performance than single material packaging **(Fig. 1.2)**. In multilayer

packaging, each thin layer fulfills a specific role (e.g., oxygen barrier, structural layer, etc.), resulting in a final material that has multiple beneficial properties without being too heavy or bulky[10]. The multiple-component nature of this packaging makes it difficult if not impossible to recycle with current, mechanical recycling infrastructure[11].

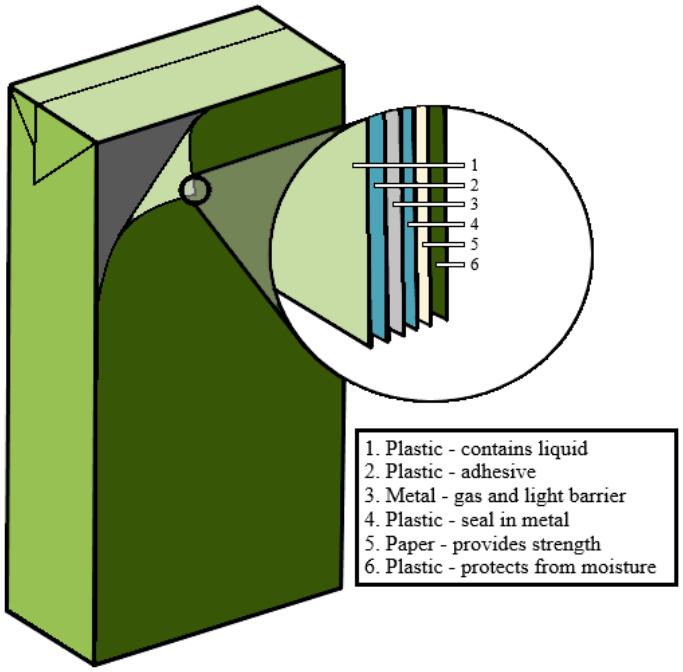

Figure 1.2. Schematic of a Tetrapak multilayer package. (Adapted from Bekhta et al., 2016)

Fortunately, plastic products are becoming more sustainable. Between legislative efforts to eliminate plastic waste and pressure from consumers, many companies have made changes to the types of plastics they are using. Unilever has started incorporating more recycled plastic resins in its products in an effort to halve its use of virgin plastic by 2025[12]. The market for biodegradable plastic resins is growing at a rate of 13.3%[13]. Polylactic acid (PLA), polybutylene adipate terephathalate (PBAT), polybutylene succinate (PBS), and polyhydroxyalkanoates (PHAs) are all considered biodegradable and/or compostable plastics. The most widely used bioplastic is PLA however, this material does not degrade any more quickly than conventional plastics in marine conditions[14,15]. As such, there is a need for multilayer packaging components that have

performance similar to (if not exceeding) their traditional, petroleum-based counterparts while being more sustainable and potentially biodegradable.

1.3 Biopolymers as a Solution

The utilization of biopolymers offer a unique solution to the plastic waste problem. Biopolymers are polymeric materials that are either produced naturally by living organisms such as proteins and polysaccharides or synthesized from chemicals derived from organisms such as PLA. Wood itself is principally made of three different biopolymers: cellulose, lignin, and hemicellulose. The cellulose extracted from wood was first used as paper in ancient China and at first was considered a luxury good. Paper was not used to make structural packaging until the early 1800s in the form of a paperboard box. The modern corrugated box was not developed until the 1850s[16]. While many modern plastics were discovered in the 1800s, they did not get used as food packaging materials until the mid-20th century and from here, the industry boomed eventually leading to the plastic waste crisis we face today.

Given the history of paper in combination with the accumulation of and reliance on petroleum-based plastic packaging, it is natural that researchers would return to the realm of biomaterials for a solution. One of the first biomaterials intentionally combined with plastic packaging films to improve its biodegradability was starch. By the early 1990s there were at least twelve commercially available petroleum-based plastic films that had at least some added starch content[17]. Research from this time shows concern with the biodegradability of these films, concluding in many cases that only the starch component was subject to any kind of degradation[17–19]. Other researchers looked at developing synthetic polymers from renewable resources. PLA is among the best and most widely used examples of a synthetic, bio-based plastic. It is formed from the ring-opening polymerization of lactide that can be synthesized from lactic acid sourced from

the fermentation of sugar cane or other high-sugar-content crops[20] (**Fig. 1.3**). Unfortunately, both of these solutions rely heavily on crops that are used as food and feed sources, which hinders their

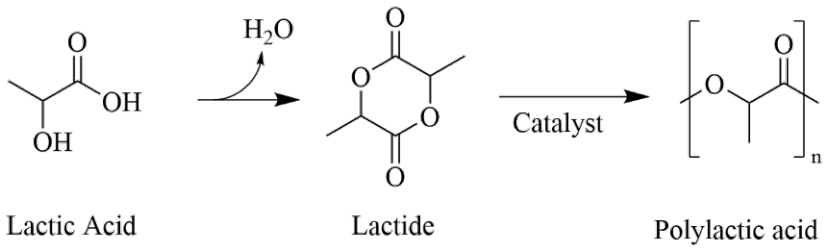

Figure 1.3 PLA synthesis from the ring-opening polymerization of lactide

sustainability. This among other limitations, including the slow and/or incomplete biodegradation of both PLA and starch-doped traditional plastics, forces us to look elsewhere for solutions.

1.3.1 Biopolymers as Water Barriers

One of the most important purposes of food packaging is to protect the food product from outside moisture both in liquid and vapor form. There are many biopolymers that are water resistant (e.g. beeswax), but they suffer from being in limited supply, mechanically weak, or otherwise inappropriate for food packaging. A composite materials approach allows researchers to combine biopolymers and other materials in such a way that they behave synergistically.

The most abundant biomaterial on the planet is cellulose and it is extracted in a relatively pure form through the paper making process. Within wood, cellulose exists in fibers that exhibit a hierarchical structure. The individual cellulose chains are combined in elementary fibrils with a diameter of 3-4 nm. These elementary fibrils are then combined into cellulose microfibrils that are embedded in a lignin and hemicellulose matrix to form the cell walls within the wood. It is possible to break down this hierarchal structure of cellulose fibers and obtain nanoscale cellulose. This class of nanomaterials is referred to as cellulose nanomaterials. To be considered a cellulose nanomaterial at least on dimension of the cellulose particle must be nanoscale (<100 nm)[21]. Cellulose nanomaterials are an expanding area of research due to the unique properties cellulose

exhibits on the nanoscale. Many cellulose nanomaterials meet the requirements of a new food packaging material (availability, mechanical strength, oxygen barrier, etc.) however they have a critical flaw—water resistance[22]. Cellulose is highly hydrophilic. The large concentration of hydroxyl groups at the surface of the cellulose allows for extensive interaction with water. This is further exacerbated at the nanoscale as the surface area of the cellulose is so greatly expanded allowing for the creating of hydrogels with greater than 99% water content by weight[21]. Bacterial nanocellulose is a type of cellulose nanomaterial that is particularly interesting for food packaging applications because it is generally recognized as safe by the FDA and is approved for food contact[23].

Bacterial nanocellulose (BC) is produced by many different species of aerobic bacteria. The bacteria excrete a series of nanofibrils which aggregate into ribbons that are approximately 70 – 150 nm wide[24]. The reason that bacteria produce this cellulose is still not completely clear with explanations including protection from UV radiation and a network through which the bacteria can more easily access oxygen at the air-liquid interface[25]. While BC is structurally different from plant-based cellulose it is chemically identical in that it is made up of β-d-glucopyranose repeat units connected by β-1,4-glycosidic linkages[24,26,27]. In contrast to plant-based cellulose, BC is produced in a pure form and therefore does not contain the lignin, hemicelluloses, and other compounds that are typically removed during the pulping process. As such the only purification needed to obtain pure cellulose is the removal of any remaining dead bacteria and growth medium which can be accomplished by treatment with a dilute alkaline solution such as sodium hydroxide (NaOH)[24,28].

BC is a byproduct of many common fermentation processes including that of kombucha and many different types of vinegar. It is also commonly eaten as a dessert in the form of *nata-de-*

coco throughout Southeast Asia. BC has also found non-food uses including as wound dressings[29], acoustic membranes[28], and more recently as a leather alternative in the fashion industry[30]. The use of BC as in the packaging industry is a growing field of research due to its unique properties[24]. Researchers are using both native BC membranes and disintegrated BC in combination with petroleum-based polymers[31–33], other biomaterials[34–36], and minerals[37–39] to make films and coatings. As is the case with plant-based cellulose, the inherent hydrophilicity of cellulose is one of the biggest challenges that must be overcome for BC to be practically used as a packaging material. If BC is going to be used as a food packaging films, they must be combined with another material to achieve the required water barrier properties.

In multilayer packaging, a single component is not responsible for the entirety of the barrier properties of the packaging as a whole. The addition of coatings between layers provide not only adhesion but can contribute to the water barrier properties as well. A fully bio-based coating that can attach to an existing multilayer component would reduce the total amount of petroleum-derived materials in the packaging. Furthermore, with the biodegradation potential of biomaterials, a bio-based coating could improve the separability of layers with incompatible recycling pathways. Lignin is another readily available biopolymer that has attractive qualities for use as a barrier layer in multilayer packaging.

Lignin exists within woody biomass alongside cellulose and is extracted during the pulping process at paper mills. Kraft lignin is of interest in the realm of packaging for many reasons including its water resistance[40]. However, lignin is a brittle solid and if used as a barrier layer alone would develop cracks and flaws that would allow moisture and gasses into the package. The answer again may be the development of a composite material that endows some beneficial mechanical properties to the lignin such that a continuous coating is possible.

Lignin is an exceptionally complex network polymer found in trees and other sources of plant-based cellulose. Lignin is removed from the cellulose fibers during the pulping process and the final chemistry of the lignin is dependent on both the species of wood and the pulping process used. As such, lignin, in both its native and technical forms, as a heterogeneous material with a structure that is variable and difficult to define[41]. The repeat units of lignin are phenylpropanoids that are derived from three precursors, sinapyl, coniferyl, and *p*-coumaryl alcohols **(Fig 1.4)**. The presence and relative amounts of each of these phenylpropanoids vary widely from species to species. The lignin used in this work was obtained from a kraft pulping process of a single species

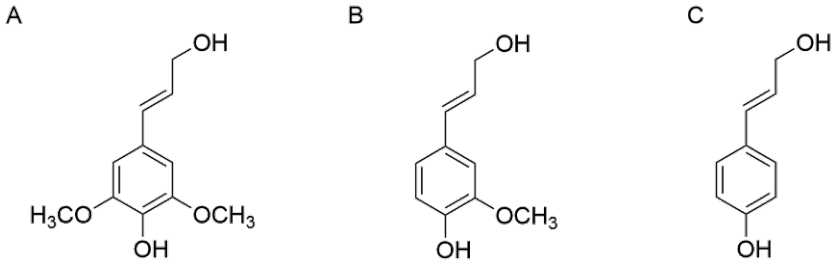

Figure 1.4. Lignin precursors A) sinapyl alcohol, B) coniferyl alcohol, C) *p*-coumaryl alcohol

of southern pine. The kraft pulping process has endowed the lignin with thiol groups in various locations.

Currently, most of the lignin extracted during the pulping process is burned for energy. However, lignin and lignin valorization has been the subject of extensive research of late. Lignin is being investigated for use as a source of high-value commodity chemicals, as a packaging material, as a nanomaterial and many other potential applications[40,42,43].

1.4 Current Bacterial Nanocellulose and Lignin Barrier Layers

Hereinafter is a brief literature review of recent research related to bacterial nanocellulose composite films and lignin composite barrier coatings. The scope of the review is limited as follows:

1. No synthetic or inorganic components are present in the films/coatings. Exceptions are made for small additions intended for antimicrobial properties (i.e., silver ions).
2. Bacterial Nanocellulose is the main component of the films (>50%).
3. Impact on water barrier properties is reported in the study.

1.4.1 Bacterial Nanocellulose Composite Films

In the literature, there are three main categories of fabrication of composite films. One, the other components are incorporated into the growth medium. Two, other components are absorbed into the bacterial cellulose membrane by soaking. Three, the bacterial cellulose membrane is disintegrated before forming the composite.

Many of the films that were modified via changes to the culture medium showed increased water absorption indicating an increased affinity for water. When water vapor permeability was assessed, the permeability increased which follows an increased affinity for water. These studies include the addition of aloe-vera gel[44], chitin/chitosan[45,46], alginate[47,48], and chemically modified cellulose[47,49]. All of these materials contain or are polysaccharides with a high concentration of polar hydroxyl groups within them. The types of materials used when altering the culture material are limited as they must be water soluble to be incorporated into the growing film. One study of note showed that the addition of curcumin to a bacterial cellulose/cotton composite showed decreased the water absorption of the films[50]. In this study, a three-layer film was formed with cotton fibers in the center and bacterial cellulose grown around it. The curcumin was added by soaking the films in an ethanol/curcumin solution at various w/v ratios. As the curcumin content increased, the films were less soluble and swelled less. As curcumin is hydrophobic, it follows that the addition of a hydrophobic substance to the BC films, even if it simply absorbed rather than grafted, can improve the water barrier properties of the film.

Similarly, the studies where the membrane was soaked after biosynthesis focused on the addition of a secondary biopolymer to the BC network with the goal of increasing the wet-strength and water retention of the BC films. The goal of this is to develop films for wound healing, not food packaging. However, understanding the interaction between these biopolymers may shed light on behaviors that could make the films more suitable for a water barrier application. Soaking existing BC films in chitosan[51–53], gelatin[54], and alginate[55] universally showed an increase in swelling and water-holding capacity. In the cellulose-alginate system, the addition of the alginate improved the mechanical properties of BC in the wet state. In this case, the alginate was added in the form of calcium alginate. Alginate has been shown crosslink in the presence of divalent metal cations like calcium so the increase in wet strength are likely due to this behavior[56–58].

The type of materials used in combination with BC were more varied when the BC was disintegrated rather than kept in its native state. Of note was the addition of several different types of protein and protein derivatives including gelatin[59] and zein[60] as well as polysaccharides like pectin[61], cashew gum[62] and modified cellulose[63–66]. Of interest is the addition of zein as it drastically increased the contact angle even at very small (<2 w%) additions[60]. As was noted above the addition of curcumin, a small hydrophobic molecule, improved the barrier properties of the BC films. Zein is similarly hydrophobic but is a much larger protein. The authors show that this increase in contact angle is due primarily to an increase in surface roughness due to the formation of uniformly dispersed zein aggregates.

1.4.2 Lignin Coatings

Lignin valorization is a popular area of research, but its application can be limited due to its mechanical properties. As such, much work has gone into the chemical functionalization of lignin for different purposes. In terms of fully bio-based modification, this has been primarily in the form of esterification with fatty acids to produce barrier coatings[67]. This esterification is

typically performed on organosolv lignin rather than kraft lignin due to its solubility. However, kraft lignin esterified with acetate, laurate and palmitate fatty acids show decreasing water vapor permeability and oxygen permeability with increasing fatty acid chain length[68]. Similarly, kraft lignin was esterified with tall oil fatty acids resulting in decreased water vapor transmission rates[69].

1.4.3 Identified Research Gaps

BC composite films have been studied but the goal of these studies is typically to increase water uptake and retention for use in the biomedical field. When studies were found that did show an increase in water resistance, (even when not the goal of the study) did so by the addition of hydrophobic molecules to the BC matrix (e.g., curcumin and zein). The addition of these hydrophobic components is always accomplished using an organic solvent. Multiple studies showed that the addition of alginate to a BC film changed the mechanical properties but this change was always accompanied by an increase in water uptake.

Fully bio-based BC composite film for food packaging applications without the use of an organic solvent have not developed. No studies consider a system with more than two non-synthetic biopolymer components. Furthermore, while the studies do attribute the observed properties to the structure and arrangement of the components within the film, none were found that developed a cohesive model of arrangement that could be used to predict the properties of future films.

Very little research has been done on the application of kraft lignin as the main component of a barrier coating and of these, none were found that focused on food packaging applications[68–70]. The combination of lignin with purified fatty acids did decrease the water vapor permeability of an applied coating but these fatty acids require an extraction process that can be expensive. There are no studies that attempt to develop lignin-based coatings with more readily available biomolecules for food packaging applications.

1.5 Research Goals

Chapter 2 of this thesis investigates the structure-property relationships within composite films containing bacterial nanocellulose, alginate and zein. The guiding questions of this project were as follows:

1. How does the addition of a predominantly hydrophobic biopolymer (zein) influence the mechanical and water barrier properties of BC films?
2. Can alginate be used to improve strength of BC while avoiding detrimental impacts on the water resistance of the film – potentially through ionic crosslinking?
3. Does a ternary system of BC, alginate, and zein behave synergistically with or without ionic crosslinking?
4. Can a conceptual model of assembly of BC, alginate, and zein be developed to explain the observed properties of the ternary composite films?

Chapter 3 of this thesis focuses on the augmentation of the water barrier properties of commercial plastic packaging films with a bio-based coating of lignin soy lecithin. The guiding questions of this project were as follows:

1. Can lignin and soy lecithin be chemically linked rather than simply mixed?
2. Does coating with a lignin/soy lecithin formulation reduce the water vapor permeability of a coated packaging substrate?
3. How does the solids content of the coating formulation influence the water vapor permeability of the coated packaging substrate?
4. Does the addition of a plasticizer enhance the modification of water vapor permeability?

1.6 Additional Selected Materials

In this research alginate, zein, and soy lecithin are combined with either BC or kraft lignin to form barrier layer. The properties and structure of these three additional materials are detailed below.

1.6.1 Zein

Zein accounts for approximately 50% of the protein in corn and is extracted from the endosperm of the corn kernels. Zein is a globular, amphiphilic protein and possess many interesting properties due to its high levels of non-polar amino acid residues. This high level of hydrophobic character makes zein insoluble in water. It is however soluble in aqueous alcohol mixtures, anionic detergents, high concentrations of urea, and at elevated pH values (pH 11 and above)[71,72]. The conformation and aggregation of zein changes based on the solvent system used. This self-assembly within solution as well as the self-assembly upon evaporation can expose hydrophobic or hydrophilic surfaces of the zein structure and therefore impact the properties of the resulting material[73]. This research presented in this work solubilizes the zein by increasing the pH of the system to approximately 12. It is suggested that this allows the zein to solubilize by converting the asparagine and glutamine residues to aspartic and glutamic acid via a deamidation reaction[74] (**Fig 1.5)**.

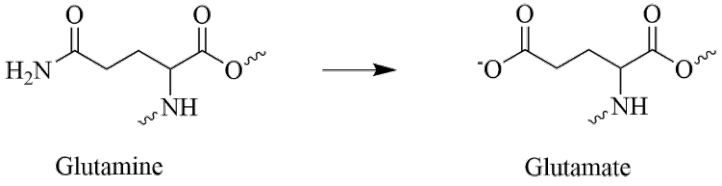

Figure 1.5 Gultamine to glutamine deamidation at alkaline pH.

Zein is not typically used as a food product, but can be found in edible coatings for pills as well as adhesives and other coating applications. Zein does naturally form films, but without the addition of a plasticizer or cross-linking agent, these films are exceedingly brittle[71,72]. This film

forming ability has prompted research into the use of zein and zein composites as petroleum-based plastic alternatives.

1.6.2 Alginate

Alginate is a water-soluble linear polysaccharide produced by seaweed. It consists of α-L guluronic acids and β-D mannuronic acids connected via glycosidic linkages. There is no specified order to the sequence of guluronic acid and mannuronic acid within the alginate chain resulting in "G-blocks" where there are only α-L guluronic acids, "M-blocks" where there are only β-D mannuronic acids, as well as sections of more random, alternating arrangements **(Fig. 1.6)**.

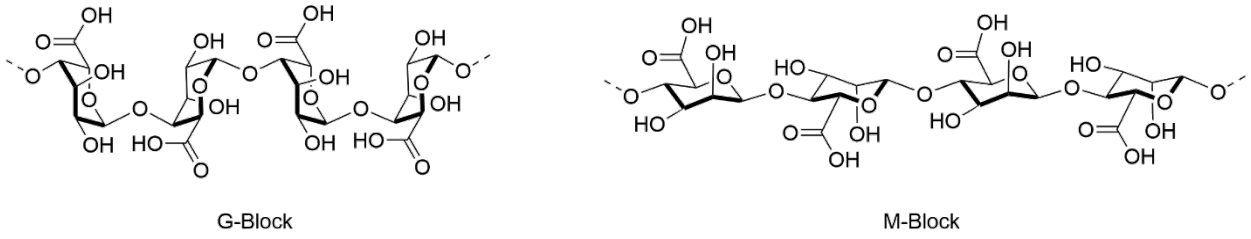

Figure 1.6. G-Block and M-Block of alginate.

Alginate exists in nature as described above, but is typically purchased as alginic acid sodium salt (i.e., sodium alginate). This molecule is largely the same with the carboxylic acid groups having sodium as the counter ion rather than hydrogen. Alginate is particularly interesting because it can be ionically crosslinked in the presence of divalent cations. This crosslinking can be explained via the egg-box model **(Fig. 1.7)** in which the divalent cations nest within G-blocks

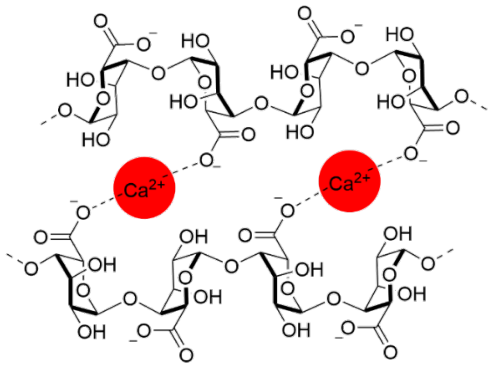

Figure 1.7. Ionic crosslinking of two adjacent alginate G-Blocks with divalent calcium ions.

on neighboring alginate molecules[75]. It should be noted that this model, while elegant in its explanation, is not universally accepted[76,77].

1.6.3 Soybean Lecithin

Soybean lecithin is a mixture of phospholipids, triglycerides and small amounts of other natural products[78]. The phospholipid portion of lecithin, specifically phosphatidylcholine, is of interest to the work presented in this thesis. Soybean lecithin is obtained from the degumming process of crude soybean oil[78,79]. It must be removed from the oil product because its emulsifier properties negatively impact oil yields and its thermal instability causes the oils to darken[80].

Phosphatidylcholine is interesting from a chemical perspective because of the classical surfactant nature of its structure. It has a zwitterionic phosphatidylcholine polar head-group and long, non-polar, fatty acid tails with varying degrees of unsaturation **(Fig.1.8)**. The reported fatty acid content of soybean lecithin varies between sources, but all agree that it contains significant amounts of palmitic (16:0), stearic (18:0), oleic (18:1), and linoleic (18:2)[78,81,82].

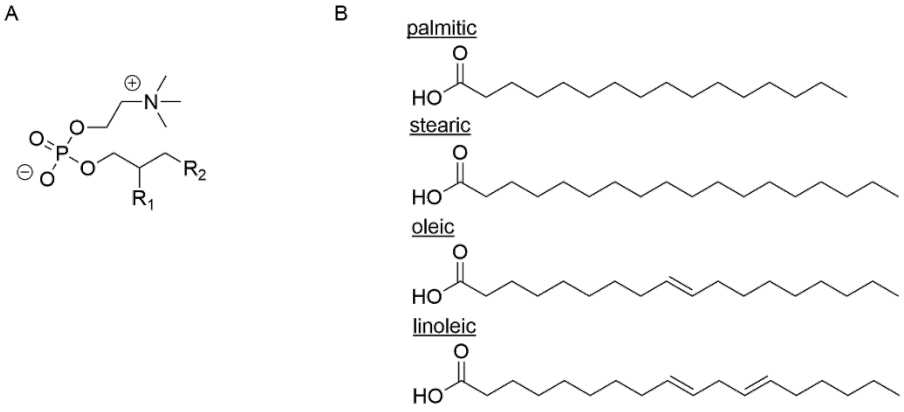

Figure 1.8. A) Phosphatidylcholine head-group where R1 and R_2 are the fatty acid tails and B) common fatty acid tails of soy lecithin.

Soy lecithins have a litany of commercial uses including as emulsifiers, food additives, release agents, adsorbents, coatings, and many more[79]. Modified soybean lecithins are being researched for use as dispersants for oil spill remediation[83–85], drug absorption aids[86–88], and diluents for cryopreservation[89–91] among other things.

CHAPTER 2: Ternary Bacterial Nanocellulose Composite Films

2.1 Abstract

Bacterial nanocellulose (BC) has been of interest in the field of sustainable packaging because of its advantageous properties such as mechanical strength. However, as a cellulosic material, BC's hydrophilicity is a roadblock to many packaging applications. In this work, ternary composite films of BC, alginate, and zein were created to increase the water barrier performance of BC while maintaining its mechanical performance. To accomplish this, the mechanical and barrier performance of two-component systems of BC/alginate and BC/zein were studied with and without ionic crosslinking. Thee-component films were developed at the weight ratios that showed the best performance. The three-component films showed improved elongation at break and water contact angle along with an increase in absorption while maintaining strength of neat bacterial cellulose films. The performance of the three-component system with ionic crosslinking was similar, however the crosslinking also increased the water vapor permeability and returned the absorption to that of neat BC. These properties can be explained with a model of assembly that includes an interpenetrating network of BC and alginate with the protein either adhering to the cellulose surface or aggregating into spheres in a void filling capacity depending on the presence of the ionic crosslinker.

2.2 Introduction

In 2018 almost 14.5 million tons of plastic container and packaging waste was produced in the United States alone. Of this 14.5 million tons, nearly 70 % was sent to the landfill[7]. Much of this landfilled plastic packaging waste is in the form of thin films as they are not easily recycled by the recycling technologies available at the municipal level and are often considered a containment in bulk recycling streams[11]. These plastic films can be stand-alone products or part of multilayer packaging. The role that plastic films fill in packaging is unique in that they augment mechanical and barrier properties while remaining lightweight and flexible. As such, there is need for a more sustainable alternative to plastic packaging films.

Biomaterials are an interesting solution to this problem. Bacterial nanocellulose (BC) in particular has garnered significant research interest recently due to its unique properties including its ability to augment the mechanical strength of composite films. BC is chemically identical to vegetal cellulose in that it consists of β-D-glucose repeat units linked by 1,4-glycosidic bonds[28]. Since BC is synthesized by bacteria, it is free of other molecules that are often present in plant-based nanocellulose, namely lignin and hemicelluloses, and could potentially require a less chemical and energy intensive process to obtain[92].

Although BC has many properties that are promising for use in packaging, the bulk of current research is on the potential use of BC in biomedical applications[24]. This is most likely due to the challenge presented by the inherent hydrophilicity of the material, which is less of a concern in the biomedical field. In an attempt to develop a material that can be used in packaging applications, BC has been used as a component in composite films containing other biomolecules[36,93,94], petroleum based polymers[31–33], and inorganic materials[37–39]. However, if the goal is to create a sustainable material, petroleum-based polymers and inorganic materials are not the best options due to the environmental impact of resource extraction. A fully bio-sourced film

based on BC has the potential to serve as an environmentally friendly, high performance, plastic-like film. This work concentrates on the addition of two other biomolecules, alginate and zein, to a primary matrix of BC.

Alginate is an algal polysaccharide consisting of β-D-mannuronic acid (M) and α-L-guluronic acid (G) residues connected by 1,4-glycosidic linkages[95]. It is extracted from seaweed using an alkaline process and is commonly used as alginic acid and alginic acid salts[96]. Nanocellulose and alginate composite films have been found to have improved mechanical and barrier performance when compared to nanocellulose films alone, especially when the alginate is crosslinked with divalent ions[57,97]. It has been hypothesized that this is due to a dual interpenetrating network formed between the nanocellulose fibers and the alginate that is then locked into place with the divalent ions[57,97]. This ionic crosslinking is commonly explained using the "egg-box" model wherein the divalent ion forms a coordination complex with the carboxylic acid groups present in the GG blocks of alginate[75]. It has been suggested that, as a load is applied to the nanocellulose and alginate composite, the crosslinked egg-box portion of the alginate disconnects and reforms allowing for the load to be transferred over a greater distance[97].

Zein and nanocellulose composites have also been developed and studied for potential application in the packing industry. Zein is an amphiphilic, amorphous polymer that can be found in the endosperm of corn[71]. It has been found that soaking BC films in low concentration solutions of zein protein (<1 wt%) greatly increased the water contact angle. The authors of the study hypothesized that this was due to an increase in the surface roughness of the films[60]. However, given the amphiphilic nature of the protein with greater that 50% hydrophobic amino acid residues, it is possible that the use of zein in a film could increase the net hydrophobic character and augment the water barrier properties in this manner.

The present study investigated binary systems of BC and alginate as well as BC and zein. From the results of this investigation, a ternary system of BC, alginate, and zein was developed at the weight ratios with the most promising mechanical and water barrier properties. These properties in combination with the behavior of the new the three-component films prompted the study of the chemical interplay between the three biomolecules within the films and the development of a cohesive model of arrangement of the three biopolymers. By understanding these interactions, the advantageous properties of the molecules (i.e. strength, water resistance, etc.) can be leveraged to develop a more ideal packaging substrate.

2.3 Experimental

2.3.1 Materials

Bacterial cellulose was purchased as hydrogels of nata de coco (Thai Agri Foods, Thailand). The zein and alginic acid sodium salt were purchased from Sigma Aldrich.

2.3.2 Suspension and Film Production

The sugars and preservatives were removed by first mechanically processing the hydrogels in a blender and the heating them for 20 min at 80 °C in a 0.1 M sodium hydroxide (NaOH) solution. The resulting suspension was then filtered and rinsed until the rinse water had a conductivity of less than 2 μS/cm. The BC suspension was transferred to dialysis tubing with a molecular weight cut off of 10 kD (Repligen, USA) and allowed to sit in deionized (DI) water until the pH of the water remained at 5.5 and the conductivity remained below 2 μS/cm for two consecutive water exchanges. The dialyzed suspension was passed through an aqueous counter collision system (Sugino, Japan) three times using a 100-micron nozzle with an outlet pressure of 180 MPa for further homogenization and individualization of the BC nanofibrils.

Aqueous suspensions of varying ratios of BC, alginate, and zein, such that the total solids content of the suspension remained at 0.4 w%. The pH of each suspension was elevated to 12 by

the dropwise addition of NaOH to solubilize the protein. Crosslinked films were prepared by soaking the dried films in a 1 w% solution of calcium chloride ($CaCl_2$) for 24 h. After crosslinking the films were soaked in DI water for 24 h to remove any excess salt solution. Once the films were rinsed, the excess liquid was poured out of the dishes and the films were allowed to dry at room temperature and pressure.

2.3.3 Film Characterization

The water contact angle of the composite films was measured using an SEO-Phoenix Contact Angle Analyzer (Kromtek, Malaysia) equipped with an 18-G needle. The FTA32 software (First Ten Angstroms, USA) was used for image analysis and calculation of the water contact angle. The reported values are an average of a minimum of 6 measurements across two different films.

The water vapor permeability of the films was determined according to ASTM E96. Approximately 5g of anhydrous calcium chloride ($CaCl_2$) was used as the desiccant. This process was conducted over eight hours with the change in mass being recorded every hour. For all the films, the rate at which water traversed the film became constant within the first two hours. The reported values are an average of three different films.

The water uptake of the films was determined using the Cobb method (ISO 535, TAPPI T-441). The films were conditioned for a minimum of 72 h at 23 °C and 50% RH before testing.

The mechanical performance of the films in tensile mode was obtained with a Universal Testing Machine (Instron, USA) with a crosshead displacement rate of 2 mm/min with an original displacement of 20 mm. The films were stored at 23 °C and 50% RH for a minimum of 72 H before testing under the same conditions. Film specimens were cut into 15mm x 60mm strips after conditioning but before testing. The Young's modulus, tensile strength, and elongation at break of

the films were normalized by the basis weight of each strip. The reported values are the average of a minimum of five measurements across two separate films.

The surface chemistry of the films was analyzed using a SPECS X-Ray Photoelectron Spectrometer (XPS) equipped with a PHOIBOS 150 analyzer. Survey scans were obtained for each film sample and high-resolution scans were taken of the carbon, nitrogen, and oxygen peaks of each film. Peak fitting and analysis were performed with the CasaXPS software. Cross-section images of the self-standing composite films were obtained using an FEI Veios 460L field emission scanning electron microscope (FE-SEM) using a through-the-lens low energy electron detector. The films were sputter coated with a thin layer of gold (ca 0.5 nm) prior to analysis. The working distance and acceleration voltage were 3.5 mm and 2 kV, respectively. Images were obtained at 1,500, 5,000, 10,000 and 15,000 times magnification.

The thermal stability of the composite films and controls was assessed by thermogravimetric analysis (TGA) (TA instruments, TGA Q500). The mass of each sample was held constant at 10 ± 0.5 mg. The samples were heated from 25 to 500 °C in a nitrogen atmosphere at a ramp of 10 °C/min. The flow rates of the nitrogen purge gas at the balance and sample were 40.0 mL/min and 60.0 mL/min, respectively. When heated in an air atmosphere the same conditions were used with only the identity of the sample gas being changed to air.

To test the ability of the bio-based films to withstand a commonly used industrial aseptic sterilization process, small pieces of the bio-based films were submerged for three seconds in 32 w% hydrogen peroxide (H_2O_2) that had been heated to 90°C. The films were immediately removed and placed on a Teflon surface and dried with warm air. These treated pieces were then subjected to the same thermogravimetric analysis method described above in an air atmosphere.

The statistical significance of the results of the mechanical testing, water contact angle, water absorption, and water vapor permeability results were confirmed via ANOVA followed by a Tukey's range test.

2.4 Results and Discussion

The films produced by the method described above were thin (ca. 30 μm) and translucent. SEM micrographs of the film cross sections show a generally featureless surface with some cracks or other defects that expose the internal structure of the films **(Fig. 2.1)**.

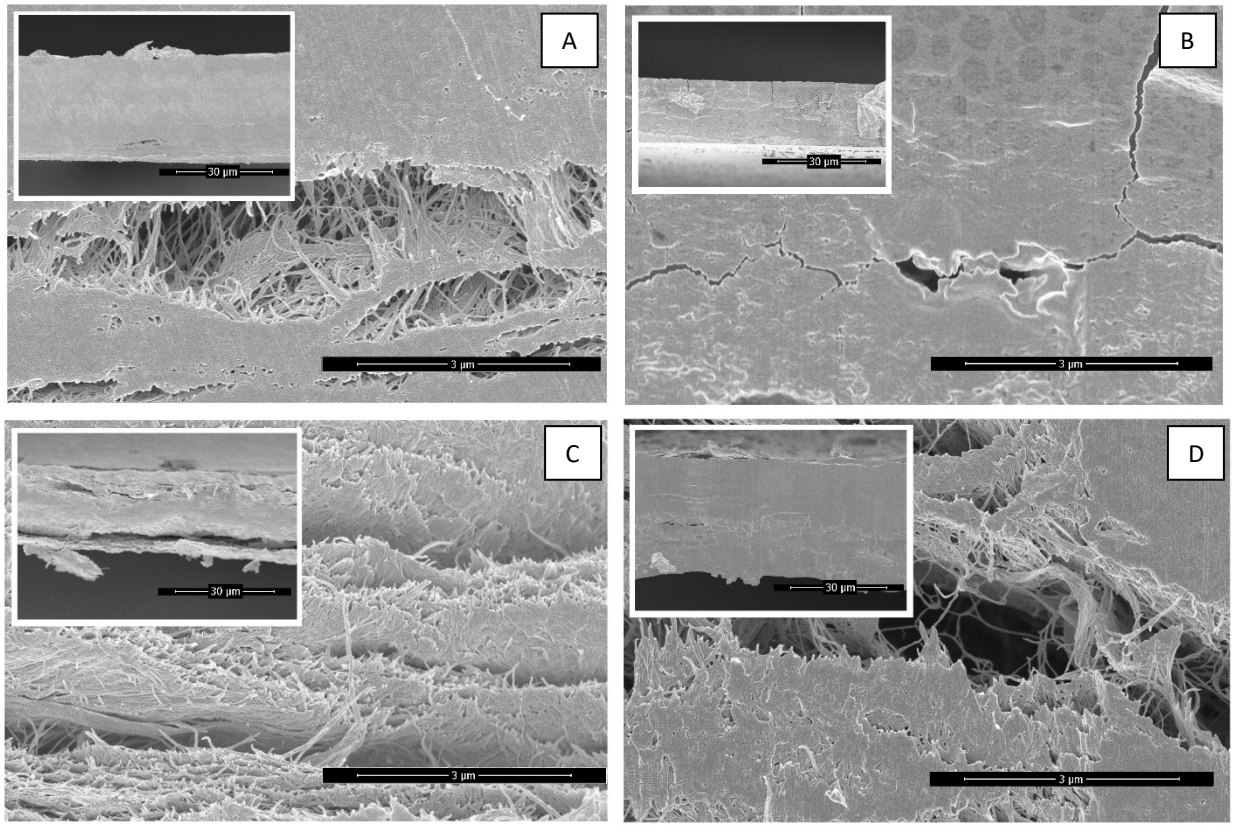

Figure 2.1. SEM micrographs of composite films at 15,000x magnification. Insets are of the same films at 1,500x magnification. (A) neat BC, (B) neat alginate, (C) 90:10 BC/A, (D) 90:10 BC/Z.

This indicates some degree of repulsion between film constituents, likely between the carboxylic acid groups on the alginate and zein and the general negative surface charge of BC. The delamination on the 90:10 BC/A films was particularly severe again likely due to the large

concentration of carboxylic acid groups on alginate. The neat alginate film does not show any fibril structure within the defects. Additionally, it is the only film to show cracks in a perpendicular direction through the film. It should be noted that the dark, spotted discoloration on the surface of the alginate films is due to over sputter coating and is not part of the alginate[98].

The addition of alginate to the BC composite films did not have a statistically significant impact on the tensile index of the films (**Fig. 2.2**). Increasing alginate content did however reduce the specific young's modulus (49%) resulting in films that are more elastic. The lack of impact on tensile index is likely due to the formation of hydrogen bonds and other weak intermolecular forces between the BC and the alginate that to replace the hydrogen bonds that are being interrupted within the BC network. The addition of zein in quantities at or above 30 w% resulted in a more

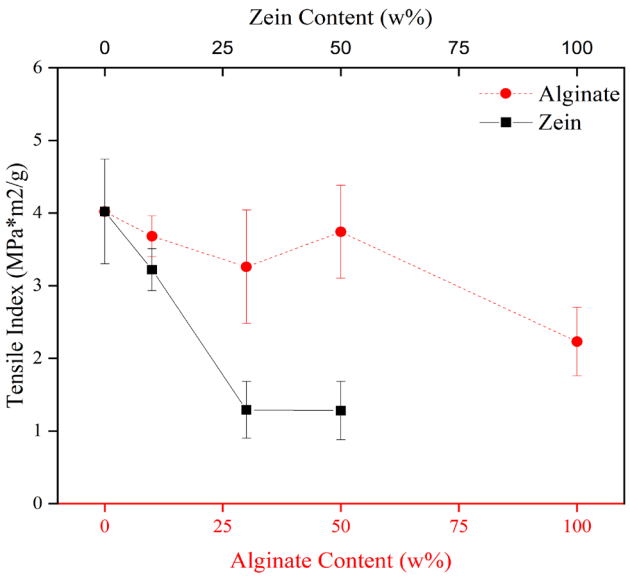

Figure 2.2. Tensile Index of uncrosslinked films at different alginate or zein content.

elastic (80%) and weaker film (68%). Furthermore, both the specific young's modulus and tensile index plateau at this point. This can be explained by understanding the method through which the zein is interacting with the cellulose. In these systems, the zein was solubilized by increasing the pH which resulted in a deamidation of the glutamine and asparagine amino acid residues the end

result of which is the presence of a new carboxylic acid group[72]. The presence of these carboxylic acid groups along with the partial unfolding of the globular protein are what allows the zein to solubilize[99]. These new carboxylic acid groups and the newly exposed hydrophilic amino acid residues from the interior of the protein allow the zein to adhere to the BC fibrils. It is likely that at 30 w% addition of zein the film is no longer being held together with the hydrogen bond interactions between adjacent BC fibrils but rather interactions between the zein adhered to the BC fibril surface. Zein is a much weaker biopolymer so the mechanical performance of the films suffers from this change. However, neat zein films were not tested because it was not possible to obtain sufficiently large samples due to its weak nature.

This proposed mechanism of assembly is further supported by the XPS data for the uncrosslinked composite films (**table 2.1**). While there is no significant change in the C/O ratio between the neat BC and 90:10 BC/Z films, high resolution C 1s scans of the films show a 30% shift from C-O bond concentration at the surface to C=O bond concentration at the surface.

Table 2.1. XPS data for representative uncrosslinked composite films.

Film	**%C**	**%O**	**%N**	**C/O ratio**	**C-C**	**C=O**	**C-O / C-N**
Neat BC	62	34	4	1.8	39	17	44
Neat Alginate	68	31	---	1.2	57	15	28
90:10 BC/A	66	34	---	1.9	56	8	37
90:10 BC/Z	62	32	5	1.9	40	47	14

* Concentration values have been corrected for carbonate contamination at the surface

This suggests that the hydroxyl groups within the cellulose are being covered by the protein, which is exposing its carbonyl functionalities at the surface. The XPS data also shows a reduction in carbonyl functionality at the surface from the neat alginate film to the 90:10 BC/A

film. This supports the idea that the carboxylate ions in the alginate are forming ion-dipole interactions with the BC and rearranging away from the surface of the film. This interaction is making up for the loss of hydrogen bonding between BC fibrils and preserving the mechanical performance of the neat BC films. It should be noted that the nitrogen content in the neat BC films is from a source of contamination on the film surface as there are no nitrogen containing groups on cellulose.

The addition of zein has no statistically significant impact on the water vapor permeability (WVP) of the films (**Fig. 2.3**).

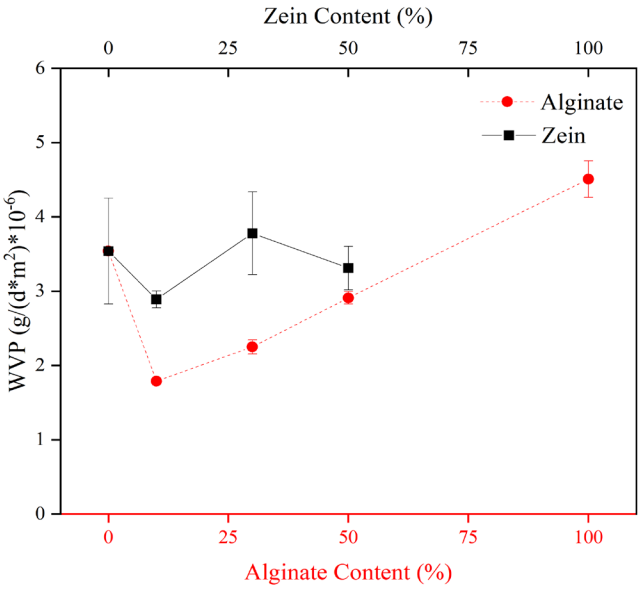

Figure 2.3. Water vapor permeability of uncrosslinked films at different alginate or zein content.

This observation fits the proposed fibril coating model as there is no aggregation of the protein in the voids that would reduce the porosity of the films. The porosity of the films does not change with the addition of zein. The addition of alginate however did significantly reduce the WVP at 10 w% as hydrophilic functional groups on the alginate form hydrogen bonds with the BC network. As more alginate is added, the WVP begins to increase again because of the increasing concentration of hydrophilic groups from the alginate within the film.

The addition of zein only significantly influences the water contact angle of the films at the 50 w% addition level and at this point the contact angle is drastically lowered. As was hypothesized above, the addition of high levels of zein may eventually be forming a continuous coating of each BC fibril. This could be resulting in a smoother surface and therefore lower contact angles. The addition of alginate immediately lowers the contact angle to that of the neat alginate films. This is caused by the presence of many free hydrophilic functional groups available to interact with water at the surface of the films.

2.4.1 Crosslinked Films

The crosslinking process influenced both the mechanical and barrier properties of the films. In general, the trends present in the uncrosslinked films remained but the values at which these trends occurred changed. Of note is the dramatic increase (ca. 100%) in the elongation at break for all of the films. For films containing alginate, this is predominantly due to the formation of a secondary interpenetrating network of alginate within the BC matrix that is "fastened" into place by interactions between the calcium ions and the carboxylate ions within the alginate. The presence of this secondary network maintains the tensile index seen in the uncrosslinked films, but results in more elastic films with greater elongation. It has been suggested that the ionic crosslinking slowly unzips which dissipates large amounts of energy while allowing the material itself to stretch before failing[97,100].

It is plausible that the change in the mechanical properties of zein is due to a similar phenomenon. The deamidation reaction of the zein resulted in an increased number of carboxylic acid groups, which would be deprotonated at the elevated working pH. These groups should be able to form ionic interactions with nearby calcium ions and form inter- and intramolecular ionic crosslinking[101]. It should be noted however that the crosslinking process also influenced the mechanical properties of the neat BC film. The specific young's modulus of the neat BC film

reduced by 67%, the tensile index reduced by 22%, and the elongation at break increased by 221% from the uncrosslinked to the crosslinked neat BC films (Supporting Information). It is unlikely that this change can be attributed to the presence of ionic crosslinking within the films as that should enhance the mechanical performance of the films. Instead, it is plausible that this change in performance is due to the drying and rewetting that occurred during the crosslinking process. The ionic crosslinking of zein containing films severely increased the water vapor permeability (**Fig. 2.4**).

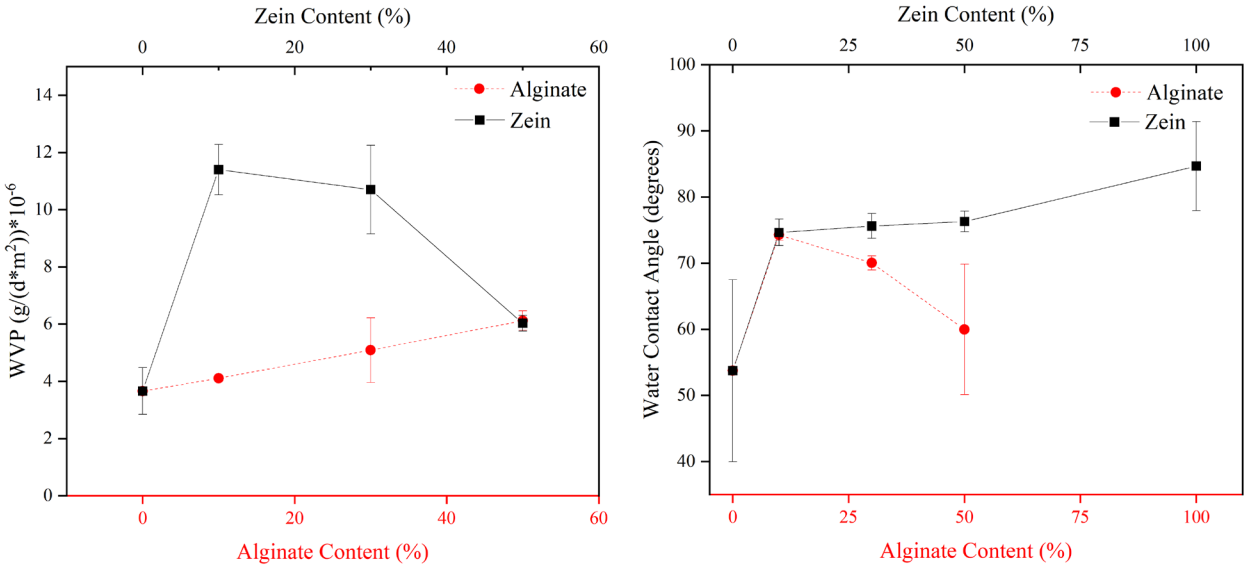

Figure 2.4. Water vapor permeability and water contact angle of crosslinked films at different alginate or zein content.

This is caused by a large increase in porosity. Since the ionic crosslinking is done after the original film is formed, the zein protein had already adhered to the surface of the cellulose fibrils. It is plausible that the introduction of calcium ions caused the zein to pull away from the cellulose in places and thereby increase the porosity. The SEM images of the crosslinked films containing zein show a spherical structure at the surface of the films (Appendix A). These spheres may be zein aggregates that formed by after ionic crosslinking. This is further corroborated by a 17% reduction

in density between the 90:10 BC/Z films and the 90:10 BC/Zx films as well as the increase in porosity (39%). This suggested arrangement is also supported by the XPS data for the crosslinked films (**table 2.2**).

Table 2.2. XPS data for representative crosslinked composite films.

Film	**%C**	**%O**	**%N**	**C/O ratio**	**C-C**	**C=O**	**C-O / C-N**
Neat BC	53	47	---	1.1	8	22	71
Neat Alginate	64	35	---	1.8	51	16	33
Neat Zein	67	23	7	2.9	84	6	11
90:10 BC/A	72	28	---	2.5	49	13	38
90:10 BC/Z	55	44	1	1.3	16	23	61

* Concentrations have been corrected for carbonate contamination. Calcium content is excluded.

In the uncrosslinked films the addition of zein to the neat BC film resulted in a shift from C-O/C-N at the surface to C=O at the surface. In the crosslinked films the C=O concentration remains roughly the same (23%) while there is a small shift from C-O/C-N to C-C. This shift accompanies a slight increase in C/O ratio showing that the total oxygen concentration at the surface is reduced. If, as suggested, the carboxylate ion is being crosslinked with the calcium and the zein is reforming into a spherical aggregate within the film then it follows that the carbonyl groups would be toward the interior of the aggregated zein rather than at the surface. This also can be supported by the low (6%) C=O concentration in the neat BC film.

The increase in contact angle with the addition of zein can be attributed to an increase in surface roughness from the aggregated zein spheres as there is still a large concentration (>61%) of hydrophilic functional groups at the surface of the 90:10 BC/Zx films. The increase and subsequent decline in contact angle with the addition of alginate can be attributed to an initial

increase in hydrophobic functionality at the surface as the C/O ratio increases to 2.5. However as more alginate is added eventually there are more free hydrophilic functional groups with which the water can interact.

2.4.2 Three Component Films

After analysis of the data for the two component films, two component films were made at the BC/A/Z weight ratio that corresponded to the most ideal performance – 80:10:10 BC/A/Z. 10 w% alginate was chosen because it resulted in the lowest WVP values (1.82 ± 0.04 (g/Pa*d*m)*10^{-6}). The choice of 10 w% zein was more complex. The WCA is the highest for 70:30 BC/Z films, but there was a noticeable negative impact on tensile index at this value. Ultimately, a compromise of 10 w% zein was chosen to increase the WCA while mitigating the loss of mechanical performance. The 80:10:10 BC/A/Z and 80:10:10 BC/A/Zx films were prepared in the same manner as the two-component films.

The 80:10:10 BC/A/Z films had a reduced tensile index (1.9 ± 0.4 MPa*m^2/g), reduced specific young's modulus (0.92 ± 0.4) and increased elongation at break (5.8 ± 0.9) when compared to the analogous films. Both the 80:10:10 BC/A/Z and 90:10 BC/Z films had increased elongation at break (ca. 130%). These changes in mechanical performance can be attributed to the overall reduction in the amount of BC in the films. It was hypothesized while studying the two-component films that the zein was coating the BC fibrils and that the alginate was forming an interpenetrating network with the BC. Assuming this model of assembly is also followed in the ternary film there are fewer locations in which the alginate can form ion-dipole interactions or hydrogen bonds with the BC as portions of the BC are obscured by the zein coating. This reduction in intermolecular forces results in a less mechanically robust film.

The water vapor permeability of the three component film remained similar to that of neat BC (3.6 ± 0.6 (g/d*m2))*10-6). Meaning that the beneficial influence of the alginate was negated

by the zein. This is again likely caused by the zein interfering with the hydrogen bond formation between the BC and alginate. If these bonds do not occur, then the amount of free hydrophilic functional groups within the film increase and are able to interact with water as it diffuses through the film. This explanation also accounts for the high absorption value of the 80:10:10 BC/A/Z films (68 ± 13 g/m^2). The addition of alginate and zein to the BC matrix had a synergistic impact on the water contact angle of the films increasing the angle more than either component did alone (75 ± 1 °). The XPS data shows an elevated C/O ratio when compared to the neat BC films (2.5 vs. 1.8) indicating less oxygen at the surface of the film as well as a high concentration of C-C bond character at the surface (72%).

A cohesive model of self-assembly for the 80:10:10 BC/A/Z films consists of an interpenetrating network of BC and alginate with zein adhered to the BC (**Fig. 2.5**).

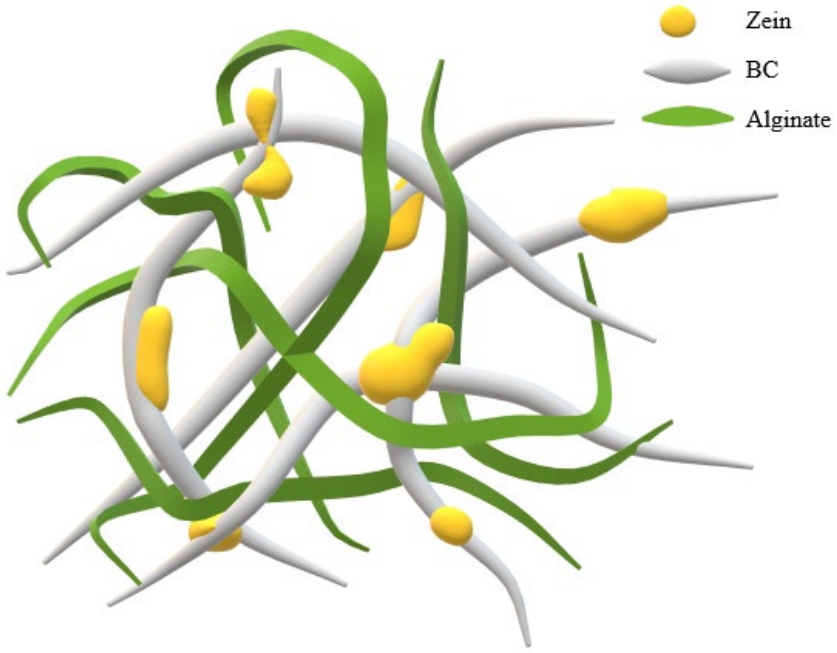

Figure 2.5. Model of self-assembly of 80:10:10 BC/A/Z films.

The BC and alginate are interacting via hydrogen bonding and ion-dipole interactions from the carboxylate ions of alginate. Similarly, since zein has undergone a deamidation reaction, the

zein is interacting with the BC via its carboxylate ions. The model of self-assembly for the 80:10:10 BC/A/Zx films differs from the uncrosslinked system in the arrangement of the zein. Rather than exist coating the BC fibrils, the zein has aggregated around calcium ions and has created voids within the films.

Ionic crosslinking with divalent calcium ions also had an impact on the performance of the three-component system. The elongation at break was similar to that of the analogous crosslinked films (6.09 ± 0.02 %). However, the tensile index (1.4 ± 0.2 MPa*m^2/g) and specific young's modulus (0.7 ± 0.1 MPa*m^2/g) decreased. This is likely caused by the reduction in the amount of BC within the system as was explained above. The WVP increased to 7.7 ± 0.6 (g/(d*m^2))*10^{-6} which can be attributed to an increase in porosity (47%) as the zein aggregates within the system. This WVP value is still lower than that of the 90:10 BC/Zx film which suggests that the presence of alginate in the system is mitigating the effect of the increase in porosity. Unlike the uncrosslinked 80:10:10 BC/A/Z films, the absorption of the 80:10:10 BC/A/Zx does not increase. This could be caused by a net reduction in the amount of free hydrophilic functional groups within the films as they are occupied by the crosslinking calcium ions. Similarly, to the uncrosslinked conditions, the addition of alginate and zein elevated the contact angle of the 80:10:10 BC/A/Zx films to 76 ± 3 °. Again, this is due to the high C/O ratio of 3 for the three-component films as well as a high concentration of C-C bond character at the surface (65%).

2.5 Conclusion – Cast Films

The three component films developed from the strategic combination of BC, alginate, and zein showed promising synergistic behavior in terms of water contact angle and were far more stretchable, especially when ionically crosslinked. The hypothesized model of self-assembly within the films allows for a deeper understanding of the forces driving the performance of the

films. Within the films, the BC and alginate form an interpenetrating network and the zein adheres to the surface of the cellulose. This arrangement shifts in the presence of a calcium ion crosslinker to one where the zein is instead forming aggregates centered around calcium ions. This shift increases the porosity of the system and affects both the mechanical and water barrier properties of the resulting films. This research demonstrates that a ternary system of BC, alginate, and zein has potential to be used as a more sustainable alternative to petroleum-based packaging films.

2.6 Vacuum Filtered Films

Composite films were also prepared via vacuum filtration as described below. Vacuum filtration was chosen to mimic the well-established paper making process. However, since the alginate and zein were completely solubilized they were not entirely caught by the membrane resulting in significant alginate and zein content in the filtrate of each film. As such, the reported weight ratios of the following films are derived from the slurry rather than the film itself.

2.6.1 Vacuum Filtered Film Preparation

Composite films were made combining BC, alginic acid sodium salt (Sigma Aldrich), and zein (Sigma Aldrich) in different weight ratios (w%). The aqueous suspensions were mixed at a total solids content of 0.4 w% and then homogenized using an Ultra-Turrax dispersing device (IKA), prior to being vacuum filtered through a hydrophobic, 0.22 μm, polyvinylidene difluoride (PVDF) membrane (Thermo Scientific). The pH of the suspensions was elevated to 12 by the dropwise addition of NaOH to allow zein to dissolve. After filtration, the films were dried under pressure at room temperature, then moved into storage at 23 °C and 50 % relative humidity (RH) for a minimum of two days prior testing **(Fig. 2.6).** Crosslinked films were prepared by pouring a 1 w% solution of calcium chloride ($CaCl_2$) over the 70:30 BC/A films and allowing it to filter

through the films (and PVDF membrane) before it was removed from the filtration assembly and allowed to dry as described above.

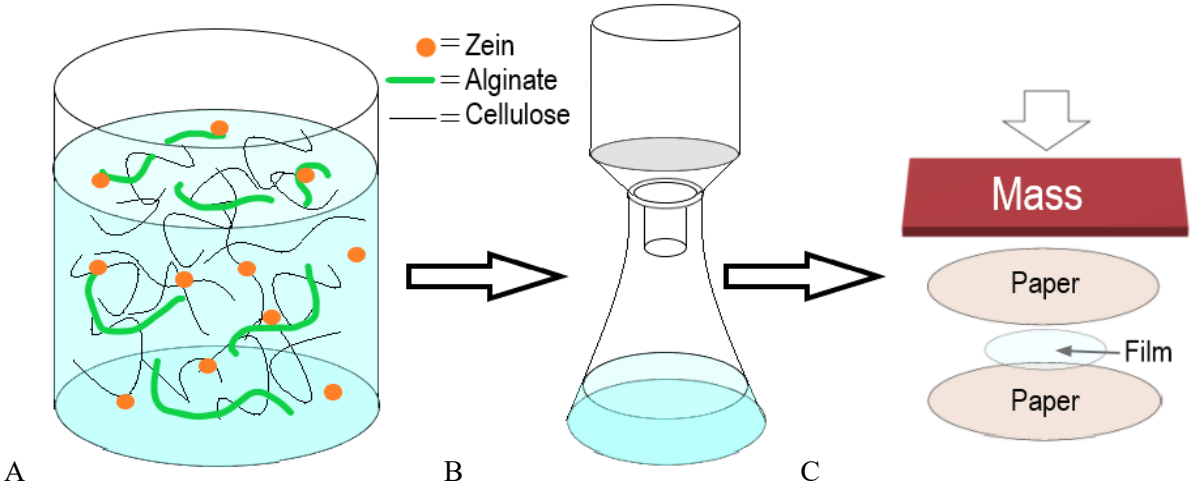

Figure 2.6. Film formation process (A) Homogeneous aqueous composite suspension, (B) Filtration process resulting in a wet cake, (C) Drying at room temperature under a mass.

2.6.2 Results and Discussion – Vacuum Filtered Films

Physical and Surface Properties

The films produced by the methods described above were translucent and flexible (**Fig. 2.7**). The films containing only BC or BC and alginate were entirely white in color, while the films containing zein had a slight yellow cast.

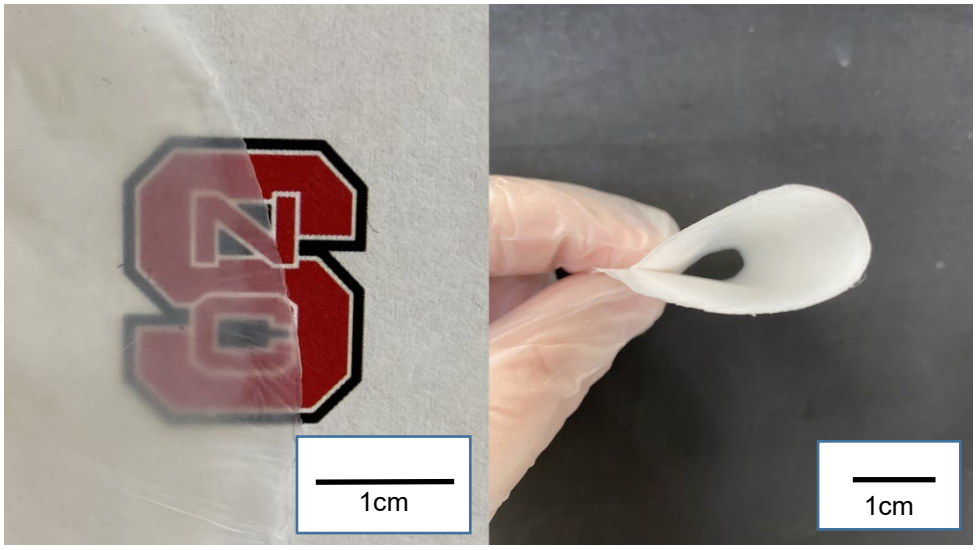

Figure 2.7. Photographs of the vacuum filtered composite films.

Figure 2.8 shows SEM images of the cross sections of the composite films. The images show dense and featureless films apart from the 70:30 BC/A film (**Fig. 2.8C)** which depicts a horizontal structure with a small degree of delamination between the layers. The 70:30 BC/A film also has a visible fiber structure at greater magnifications (Appendix A). The films containing zein show a lobed structure at the surface of the film. This lobed structure indicates that zein may be increasing the surface roughness of the films.

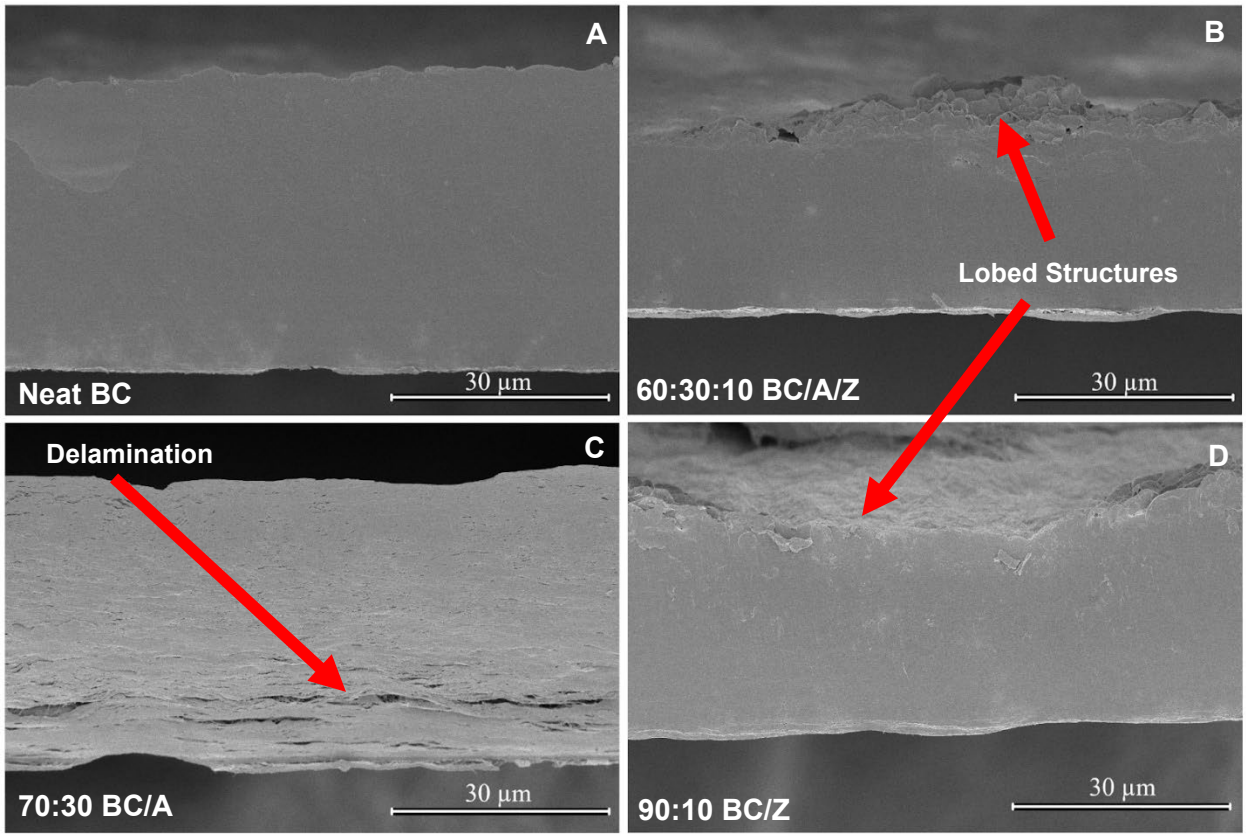

Figure 2.8. SEM micrographs of film cross sections at 1500x magnification (A) BC, (B) 60:30:10 BC/A/Z, (C) 70:30 BC/A, (D) 90:10 BC/Z.

The XPS data shows the presence of O-H bonds at the surface of all films. The films containing zein, namely the 90:10 BC/Z and 60:30:10 BC/Alginate/Zein films, also showed small nitrogen peaks (<2%) confirming the presence of the zein protein at the surface of the films

(Appendix A). This relatively low nitrogen content is evidence that not all of the zein is retained within the films during the filtration process.

The high-resolution scans of the carbon peaks show significant changes between the films. The relative amount of carbon and oxygen at the surface of the films as well as the amount of C-C, C-O, and C=O bonds are given in (**table 2.3**).

Table 2.3. XPS data for representative vacuum filtered composite films

Film	C 1s %	O 1s %	C/O ratio	C-C %	C-O %	C=O %
Neat BC	44	55	0.80	22	60	18
70:30 BC/A	60	40	1.50	34	45	21
70:30 BC/Ax	60	40	1.50	27	54	19
90:10 BC/Z	43	56	0.77	13	65	22
60:30:10 BC/A/Z	62	37	1.68	34	52	14

Of particular interest is the increase of C-C bond character and reduction of C-O in the 70:30 BC/A, 70:30 BC/Ax and 60:30:10 BC/A/Z films. This indicates that the hydrophilic –OH groups are being pulled away from the surface. This is most likely due to hydrogen bond interactions between the alginate and cellulose (**Fig. 2.9)**.

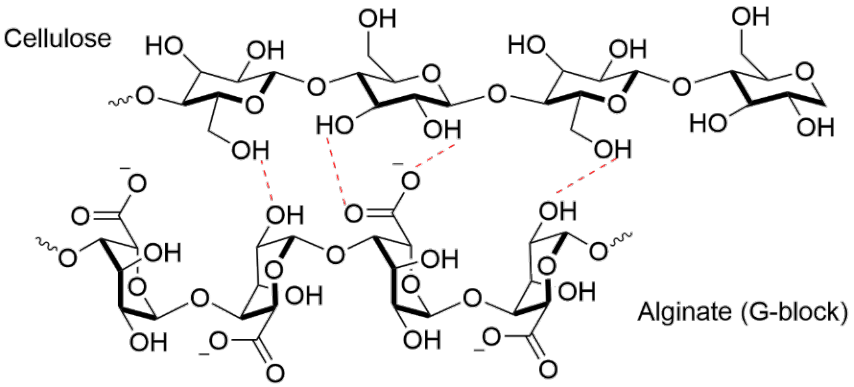

Figure 2.9. Hydrogen Bonding between Cellulose and Alginate

This is further corroborated by the decrease in oxygen at the surface of the films. The 90:10 BC/Z films show an increase in the amount of hydrophilic functional groups at the surface, especially the C=O. This, combined with the relatively low nitrogen levels at the surface (<2%), supports the idea that some of the amino acid residues in the zein are undergoing a deamidation reaction at the elevated pH here, 12. The deamidation reaction converts the primary amine ($-NH_2$) on the glutamine and asparagine amino acid residues into a carboxylic acid (-COOH) and allowing the zein to solubilize[74,102]. An additional point of interest is the synergistic effect of the addition of both zein and alginate in the 60:30:10 BC/A/Z films. The C/O ratio is the highest in these films and the concentration of C-C bonds at the surface is the same as that of the 70:30 BC/A films. The structures of alginate and zein allow for hydrogen bonding and ion-dipole interactions to form which would allow the zein to adhere to the surface of the alginate within the films.

Mechanical Performance of Composite Films

Table 2.4 shows the impact of the addition of both alginate and zein on the tensile strength, Young's modulus, and elongation at break of the BC-based films.

Table 2.4. Mechanical properties of vacuum filtered films

Film	**Tensile Index** (MPa.m^2/g)	**Specific Young's Modulus** (MPa.m^2/g)	**Elongation at Break** (%)
Neat BC	2.06 ± 0.38^{a}	0.74 ± 0.27^{a}	11.83 ± 1.78^{a}
70:30 BC/A	3.26 ± 1.00^{b}	1.86 ± 0.81^{b}	8.40 ± 1.75^{b}
90:10 BC/Z	1.76 ± 0.21^{a,c}	0.97 ± 0.16^{a,c}	7.28 ± 1.23^{b,c}
60:30:10 BC/A/Z	2.55 ± 0.70^{a-e}	1.58 ± 0.23^{b,c}	6.95 ± 2.15^{b,c}
70:30 BC/Ax	1.21 ± 0.24^{e}	0.40 ± 0.15	14.03 ± 1.85^{a}

$^{a-f}$ Values with the same superscript in the same column indicate values that are not statistically different from one another ($p > 0.05$, t-test)

Overall, there is very little difference in tensile index between the three-component films and the other films. The three-component films containing BC, alginate, and zein had the highest specific Young's modulus (1.58 ± 0.23 MPa.m^2/g), while the 70:30 BC/Ax films had the highest elongation at break (14.03 ± 1.85 %).

The mechanical performance of the 90:10 BC/Z films was similar to that of neat BC films in both tensile index and specific Young's modulus. This supports the idea that the zein self-assembled into small particles[103] rather than forming any kind of continuous supporting network. The small particles may be adhered to the surface of either polysaccharide via hydrogen bonding

or aggregating in the voids between the polysaccharides. Both the tensile index and the specific Young's modulus were higher for the 70:30 BC/A films when compared to the neat BC films by 58% and 151% respectively, while the elongation at break was lower by 29%. This reinforcing effect suggests that a secondary alginate network may have formed within the films as a support of the existing BC network[58,97,104,105].

The three-component films generally behaved as an average of the impact of the addition of zein and alginate. The tensile index that is not statistically different from that of neat BC, but the specific Young's modulus was higher (113%) and the elongation at break was lower (41%). The lack of impact on the tensile strength of the films may be due to BC remaining the primary component of the films while the change in Young's modulus and elongation at break arise out of the interruption or reinforcement of the hydrogen bonding within the cellulose itself.

The 70:30 BC/Ax films exhibited unique performance among all the films. The ionic crosslinking resulted in a lower tensile index (62%), lower specific Young's modulus (78%), and higher elongation at break (67%) when compared to its uncrosslinked counterpart. This crosslinking resulted from ionic interactions between the divalent calcium ions from the calcium chloride ($CaCl_2$) solution and the carboxylic acid groups on the alginate chains[100]. As the load was applied to the films, these linkages slowly break and dissipate the applied load rather than snapping, which resulted in the gradual elongation of the material[97]. However, this crosslinking occurs at one of the major sites of intermolecular attraction (ion-dipole) between the cellulose and alginate chains. The interruption of this connection between the materials reduces the overall tensile strength.

The goal of this work is to develop a replacement for current commercial aseptic films, and as such the properties of two commonly used commercial polymer films, low density polyethylene

(LDPE) and ethylene vinyl alcohol (EVOH), were tested and compared to the properties of the neat BC and the 60:30:10 BC/A/Z films (**table 2.5**).

Table 2.5. Comparison of mechanical properties of commercial films and BC composite films

Property	**LDPE**	**EVOH**	**Neat BC**	**60:30:10 BC/A/Z**
Tensile Index (MPa*m^2/g)	4.8 ± 0.7	5.6 ± 0.2	2.1 ± 0.38	2.6 ± 0.7
Specific Young's Modulus (MPa*m^2/g)	2.1 ± 0.2	0.6 ± 0.04	0.7 ± 0.3	1.6 ± 0.2
Elongation at Break (%)	1278 ± 117	162 ± 7	12 ± 1.78	7 ± 2

While the current films do not currently meet the performance of the commercial comparisons, significant progress has been made toward a competitive film. The 60:30:10 BC/A/Z films already outperforms the EVOH films in terms of specific Young's modulus.

Barrier Properties

The presence of zein in the films may have increased the water repellency of the films, as shown by the increase in water contact angle (**Fig. 2.10**).

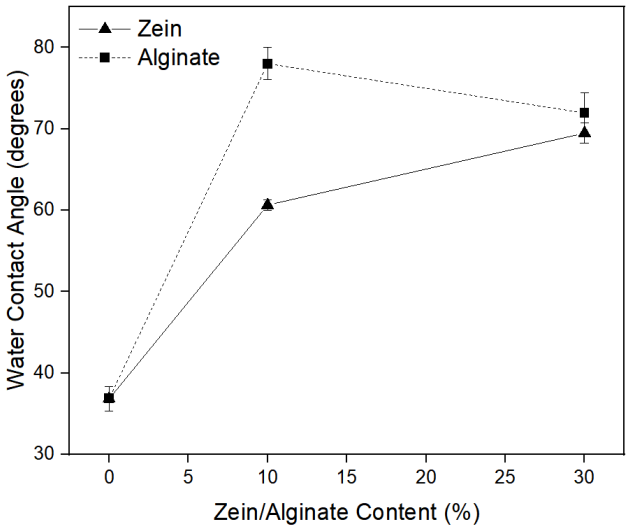

Figure 2.10. Water contact angle for films with increasing zein/alginate content

The presence of non-polar amino acids, namely leucine, alanine, and proline, in the amphiphilic structure of zein can increase the bulk water repellency of the films containing zein[71,72]. The contact angle of the zein containing films may also be increased by increasing the surface roughness of the films as was visualized on the SEM micrographs. The addition of alginate also increased the water contact angle, but since alginate is a water-soluble biopolymer, this cannot be attributed to the innate hydrophobicity of the material. The XPS data indicated an increase in the C-C bonds at the surface of the material for the 70:30 BC/A films, and a lack of the carbonyl peak one would expect given the structure of alginate. This corroborates the trend in contact angle observed. The interactions between the hydroxyl groups on the BC and the alginate result in an overall lack of hydroxyl groups on the surface as is supported by the 15% drop in oxygen concentration at the surface between the neat BC and the 70:30BC/A films. This drop in

hydrophilic surface functionality is likely responsible for the overall increase in water repellency of the composite films.

While the addition of both zein and alginate notably increased the water contact angle of the films from 37° in the neat BC films to a maximum of 78° in the 90:10 BC/Z films, the overall goal is to increase the water contact angle to beyond 90° to compete with films currently in use in aseptic packaging (e.g., polyethylene).

The water vapor permeability (WVP) data also shows improvement of the water vapor resistance of the films (**Fig. 2.11**). The decrease in water vapor permeability is likely due to the chemical and physical interaction between the three components, as described earlier. The alginate is forming a secondary interpenetrating layer with the BC in which the most hydrophilic functional groups, namely –OH, are turned toward the interior of the films rather than at the surface. These –OH groups are then occupied and not available to interact with the water vapor to facilitate its movement through the film[106].

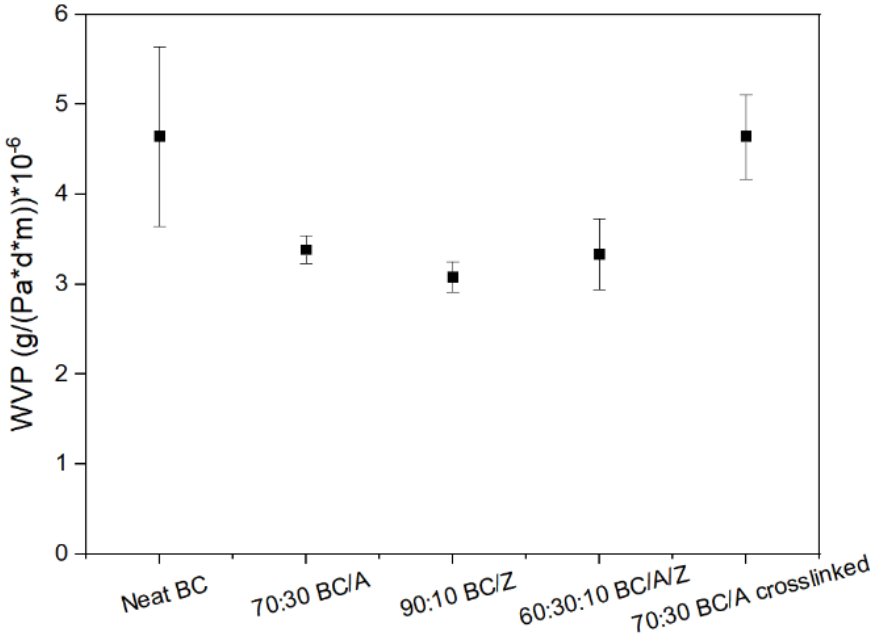

Figure 2.11. Water vapor permeability of various films.

The zein is self-assembling into particles that fill the voids within the films or adhere to the polysaccharide surface via hydrogen bonding and other intermolecular forces. This may be reducing the porosity of the films making it more difficult for the water vapor to pass through. However, the WVP of the 70:30 BC/Ax films was the same as that of the neat BC films. According to the XPS data, the crosslinked films show a smaller concentration of carbonyl groups on their surface (3%) when compared to their uncrosslinked counterpart. This supports the idea that an ionic bond has been formed during the crosslinking process between the carboxylate groups of the alginate ($-COOH^-$) and the divalent metal ions (Ca^{2+}) of the $CaCl_2$ solution. However, this ionic crosslinking occurs at the same locations within the films that the hydrogen bonding is theorized to occur in the 70:30 BC/A films that have not been crosslinked (i.e. the carboxylic acid groups on the alginate). As such, this ionic crosslinking may prevent the hydrogen bonding the BC and the carboxylic acid groups on the alginate resulting in more hydrophilic hydroxyl groups being free to interact within the bulk of the films. This may contribute to the higher WVP values because as water enters the bulk of the films it is able to interact via hydrogen bonding with these groups[106].

The water resistance properties of the neat BC and the 60:30:10 BC/Alginate/Zein films were compared to both LDPE and EVOH (**table 2.6**). While the addition of zein and alginate to the BC matrix does improve the water resistance when compared to the neat BC films, more progress must be made to meet the performance of current commercial films.

Table 2.6. Comparison of barrier properties of commercial films and BC composite films

Property	**LDPE**	**EVOH**	**Neat BC**	**60:30:10 BC/A/Z**
Water Contact Angle (°)	90 ± 3.0	91 ± 2.0	38 ± 3.0	59 ± 7.0
Water Vapor Permeability (g/(Pa*s*m))*10^{-11}	0.17	0.24	5.4 ± 1.2	3.9 ± 0.46

Heat Resistance

Thermogravimetric analysis was conducted to determine the ability of these composite films to resist the high temperatures (ca. 160 °C)[107] used in the aseptic sterilization process. BC, alginate, and zein have been shown to decompose at the fastest rate at temperatures above 200°C, thus above 160°C[71,95,108]. **Table 2.7** shows the degradation temperatures for the composite films, as well as zein and alginate standards.

Table 2.7. Thermogravimetric analysis of the composite films and controls, in an air atmosphere

Films	**$T_{5\%}$** (°C)	**$T_{10\%}$** (°C)	**DTG*** (°C)
Neat BC	139	261	299
Zein powder	70	225	277
Alginic acid sodium salt	48	80	222
70:30 BC/A	74	251	299
90:10 BC/Z	101	233	295
60:30:10 BC/A/Z	94	249	295
70:30 BC/Ax	59	194	237

*The DTG is the derivative of the weight change with regard to temperature

The temperature at which the maximum degradation occurred did not significantly change with the addition of zein and alginate to BC. However, all composite films performed better than either zein or alginate alone, remaining near the degradation temperature of neat BC (apart from the crosslinked films). This preservation of thermal integrity is possibly due to chemical and physical interactions between the composite components that bind thermally sensitive functional groups (e.g., carboxylic acids)[109]. This could be the formation of ion-dipole interactions between the carboxylic acid groups on the alginate and zein and the hydroxyl groups on the BC. The 70:30

BC/Ax films showed a large decrease in maximum degradation temperature, potentially indicating a lesser degree interaction between the BC and alginate due to the replacement of the hydrogen ion on the carboxylic acid with the calcium ion from the crosslinking solution. This is supported by the reduction in the C=O concentration at the surface of the films (2%) in the XPS data.

Most interestingly, each film type displayed only one degradation step which suggests that the biopolymers are chemically interacting with one another rather than simply existing as a mixture[110] (Appendix A).

Aseptic Resistance

The TGA data for the aseptic resistance test can be found in **Table 2.8**. In general, the temperature at maximum degradation decreased after aseptic sterilization, but remained above the temperatures used in the process (ca. 160 °C). To replicate the industrial aseptic sterilization process, films were briefly exposed to heated hydrogen peroxide and dried with hot air before further testing.

Table 2.8. Maximum degradation temperatures of films with and without aseptic treatment

Film Type	**DTG before sterilization*** (°C)	**DTG after sterilization*** (°C)
Neat BC	299.4	287.5
70:30 BC/A	298.6	294.3
90:10 BC/Z	295.0	286.1
60:30:10 BC/A/Z	294.6	306.5
70:30 BC/Ax	237.2	287.5

*The DTG is the derivative of the weight change with regard to temperature

Hydrogen peroxide is commonly used in the bleaching process by the paper industry, thus its use with bacterial cellulose was expected to alter the properties of the BC-containing films. The

sterilization process investigated in this project did change the maximum degradation temperature for both the three-component films and the cross-linked films, confirming that bacterial cellulose, alginate and zein chemically interacted with one another, in turn, creating a synergy in the film properties.

2.6.3 Conclusion

The composite films developed show enhanced water contact angle, water vapor permeability, mechanical, and thermal performance compared to neat BC, but further improvements are required to match the performance of current aseptic films. The films also show some resistance to the aseptic sterilization process. However further investigation is required to determine the impact of this process on the mechanical and barrier properties of the films.

Understanding the arrangement of the three biopolymers within the system is crucial to understanding how the properties of the films can be enhanced. As such, there are two proposed mechanisms of arrangement (**Fig. 2.12**).

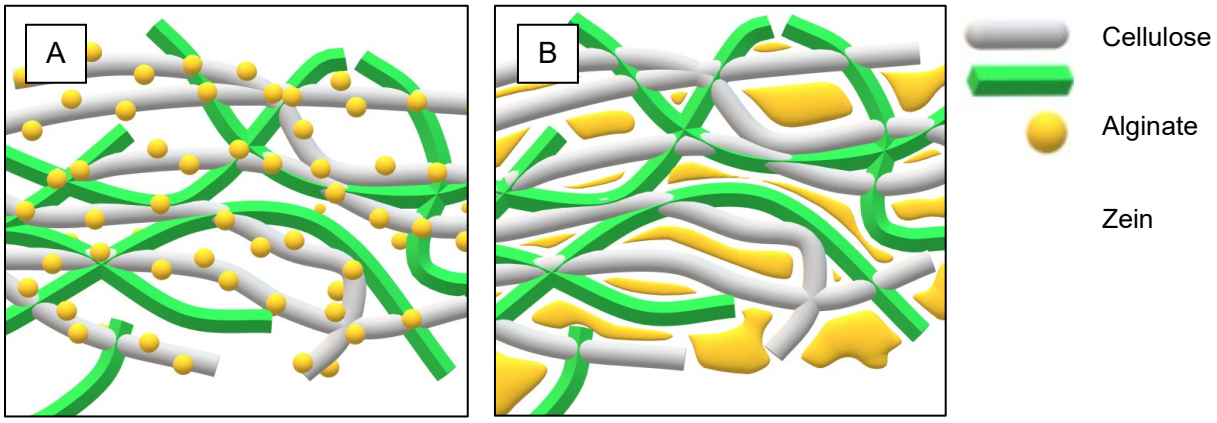

Figure 2.12. (A) Adhesion model and (B) Void filling model of film composition

Both arrangements show BC and alginate forming a dual interpenetrating network as this has been well established in the literature. The mechanism A shows the zein self-assembling into particles and adhering to the surface of the polysaccharides via hydrogen bonding and ion-dipole

interactions. The second shows the zein aggregating via those same interactions and acting in a void-filling capacity. Both of these arrangements explain the changes seen in both water barrier and mechanical performance of the films. More work will need to be done to determine the method of assembly including investigating the impact of solvation method on the conformation of zein and therefore the properties of the films. While the results from the cast and vacuum filtered films cannot be directly compared, the results for both the mechanical performance and water resistance show similar trends.

CHAPTER 3: Lignin-Based Barrier Coating for Multilayer Food Packaging Films

3.1 Introduction

Multilayer packaging has been used for decades to aid in the preservation of foods and beverages. These multilayers can consist of paper, coatings, petroleum-derived plastics, and metallic foils that work together to protect the contents while remaining lightweight and flexible. This combination of multiple types of material however is difficult to recycle due to technological limitations at the municipal level[11]. Researchers have taken many different approaches to solving this issue including developing new recycling methods, making the layers of the packaging more easily separable, and using more sustainable sources for the plastics[111–113]. Each of these approaches offers valuable improvement to the sustainability of multilayer packaging however none of them fully address the problem. How can multilayer packaging be made more sustainable in a way that will be easily implemented at the municipal level and reduce the use of petroleum-derived chemicals?

Biopolymers offer a unique solution to the presented challenge as a sustainable and potentially biodegradable tie layer between incompatibly recyclable components (namely plastic and metal) would result in simpler recycling and would not increase petrochemical usage. If this bio-based layer is sealed between the plastic and metal until the time of recycling it may be possible to delay pre-mature biodegradation. Lignin in particular has been the center of recent research due to the unique properties its predominantly aromatic structure provides. Lignin is an amorphous, thermoplastic-like, highly-branched polymer that is byproduct of the pulping process of plant-based cellulose[114]. It has an ill-defined structure due to its polydispersity, complexity, the severity of the extraction process, and that its exact makeup varies based on species and environment.

The properties of the extracted lignin vary depending on the method of pulping used. The kraft pulping process using sodium hydroxide and sodium sulfide at elevated temperatures and

pressures to break down the cellulose fibers and remove the lignin. The lignin obtained via process is a fine, brown, water-insoluble powder that is typically burned as a fuel source at the paper mill. Recent research has attempted to use lignin and lignin derivatives in packaging materials. It's ability to act as an antioxidant has made it attractive for light sensitive applications[115–117] and it's insoluble nature has been used by many to decrease the water sensitivity of some packaging materials. On its own however, lignin lacks the mechanical strength to act as a packaging material or even as a component of a multilayer as it would easily crack as the packaging was manipulated[118]. This work uses lignin in combination with soy lecithin to create a barrier coating for use in multilayer food packaging.

Soy lecithin is a phosphatidylcholine obtained from the degumming process of soybean oils. It is a natural surfactant consisting of a polar phosphocholine head group linked to two non-polar fatty acid tails via a glycerol backbone [78] (**Fig 1.8**). Soy lecithin contains varying amounts of palmitic, stearic, oleic, and linoleic acids. Of these four both oleic and linoleic acid have at least one unsaturated double bond. It is commonly used in the food industry as an emulsifier and viscosity modifier[79], but has seen more recent use as a dispersant for oil spill remediation[83,85]. The combination of soybean lecithin and lignin has not been investigated as a packaging material.

3.2 Experimental Methods

3.2.1 Materials

Kraft lignin (Biochoice™, BCL) was kingly supplied by Domtar (US) and used as received. Soybean L-α-Lecithin was purchased from Sigma Aldrich (US) and used in the epoxidation reaction. Soy lecithin that was used as a plasticizer was purchased as Performix™ E from Archer Daniels Midland (US). The formic acid, hydrogen peroxide, deuterated dimethylsulfoxide (DMSO-d6), and *p*-toluenesulfonic acid were purchased from Sigma Aldrich (US). The 2-butoxyethanol that was used as a solvent was purchased from VWR (US). The plastic films used as coating substrates were provided by an industry partner.

3.2.2 Soy Lecithin Epoxidation

The soy lecithin was epoxidized by peroxyformic acid that was formed in situ via the reaction of formic acid with concentrated hydrogen peroxide in the presence of a catalytic amount of p-toluenesulfonic acid (PTSA) (**Fig. 3.1**)[119]. The reaction was performed with a small stoichiometric excess of formic acid to unsaturated C=C bonds in the lecithin and with a 1:1 stoichiometric ratio of formic acid to hydrogen peroxide (Appendix B).

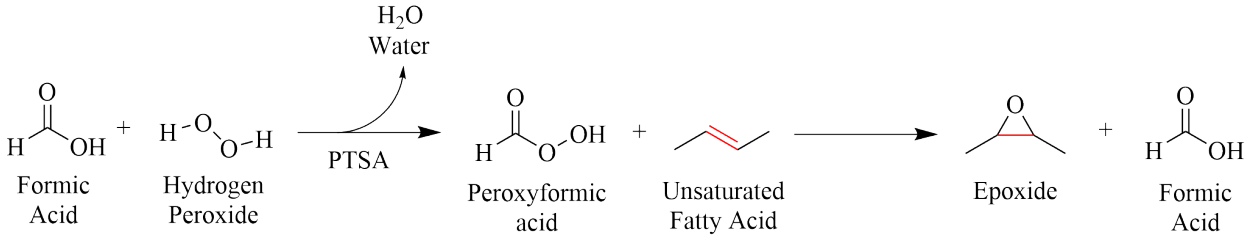

Figure 3.1. Reaction scheme of epoxidation reaction

The PTSA was dissolved in formic acid in a round bottom flask in a water bath held at 70°C. Once dissolved, the soy lecithin was added while stirring. Once the contents had reached 70°C, the hydrogen peroxide was added dropwise to the reaction vessel. This reaction is highly

exothermic so careful attention was paid to keep the temperature of the reaction below 90°C to avoid the ring-opening of the newly formed epoxide groups[119]. After the addition of the hydrogen peroxide, the reaction was continued for an additional 20 minutes to ensure complete reaction. Lastly, the reaction vessel was removed from the water bath and the contents were allowed to cool before storing in a glass vial at room temperature.

3.2.3 Epoxidized Soy Lecithin (ESL) and Lignin (BCL) Coating Formulation

Coating formulations of varying solids content, with or without the addition of plasticizer were created by reacting the ESL with BCL in a 1:1.1 stoichiometric ratio with the assumption that the product of the soy lecithin epoxidation reaction was 100% ESL and that the reaction would take place exclusively at the phenolic alcohol moieties within the BCL (Appendix B). The BCL was dissolved in 2-butoxyethanol such that a total of 20 g of coating formulation would be generated and was placed in a small beaker. The ESL was added along with a small magnetic stir bar before placing the beaker into a water bath held at 70°C for five minutes. The resulting formulations (ESL+L) were stored in plastic vials at room temperature until used.

The addition of the 2-butoxyethanol solvent modifies the viscosity of the ESL+L to a point where it can be easily coated at room temperature. The ESL+L formulation behaved in a thermoset-like fashion, only flowing at elevated temperatures. At room temperature, the ESL+L formulation without the solvent quickly cures into a hard solid hindering the coating process.

3.2.4 Coating Procedure

The plastic films were coated using a road coater and the threaded bar #8 corresponding to a coating thickness of 16μm. The coated films were dried for two days in a fume hood at room temperature.

3.2.5 Water Barrier

The water contact angle (WCA), the water vapor transmission rate (WVTR), and the water vapor permeability (WVP) were measured for each set of coated and uncoated films as well as coated and uncoated paperboard. The WCA was determined via the sessile drop method using an SEO-Phoenix Contact Angle Analyzer (Kromtek, Malaysia) equipped with an 18-G needle. The image analysis and calculations of the WCA were completed using the FTA32 software (First Ten Angstroms, USA). The reported values are the average of six measurements taken from two different places within the tested material.

The WVTR and WVP were determined according to ASTM E96. Anhydrous calcium chloride ($CaCl_2$) was used as a desiccant. The experiment was conducted for a minimum of 8 h with measurements being taken approximately every hour. Time was kept with a stopwatch and recorded down to the second. The experiment was stopped when the rate of change between measurements changed less than 5% across three different measurements. The WVTR and WVP were calculated as follows:

$$\mathrm{WVTR} = \frac{\Delta \mathrm{m}}{\Delta \mathrm{t}} \times \mathrm{S}^{-1} \quad (1)$$

$$\mathrm{WVP} = \frac{\mathrm{WVTR} \times \mathrm{l}}{\mathrm{P}} \quad (2)$$

where Δm is the change in total mass in g, Δt is the elapsed time in sec, S in the tested surface area in m^2, l is the average thickness of the tested material in m, and P is the vapor pressure of water at testing conditions in Pa. The reported values are the averages of at least two measurements.

1D ^{1}H NMR spectra were obtained using a Bruker AVANCE 500 MHz spectrophotometer. NMR data were processed with Bruker TopSpin software. The samples were prepared by dissolving approximately 30 mg of the solid sample material in 500 µL of DMSO-d6 and then transferred to a 5 mm NMR tube with a glass pipette.

3.3 Results and Discussion

3.3.1Reaction Characterization

The epoxidation reaction was characterized via 1D ^{1}H NMR (**Fig. 3.2**).

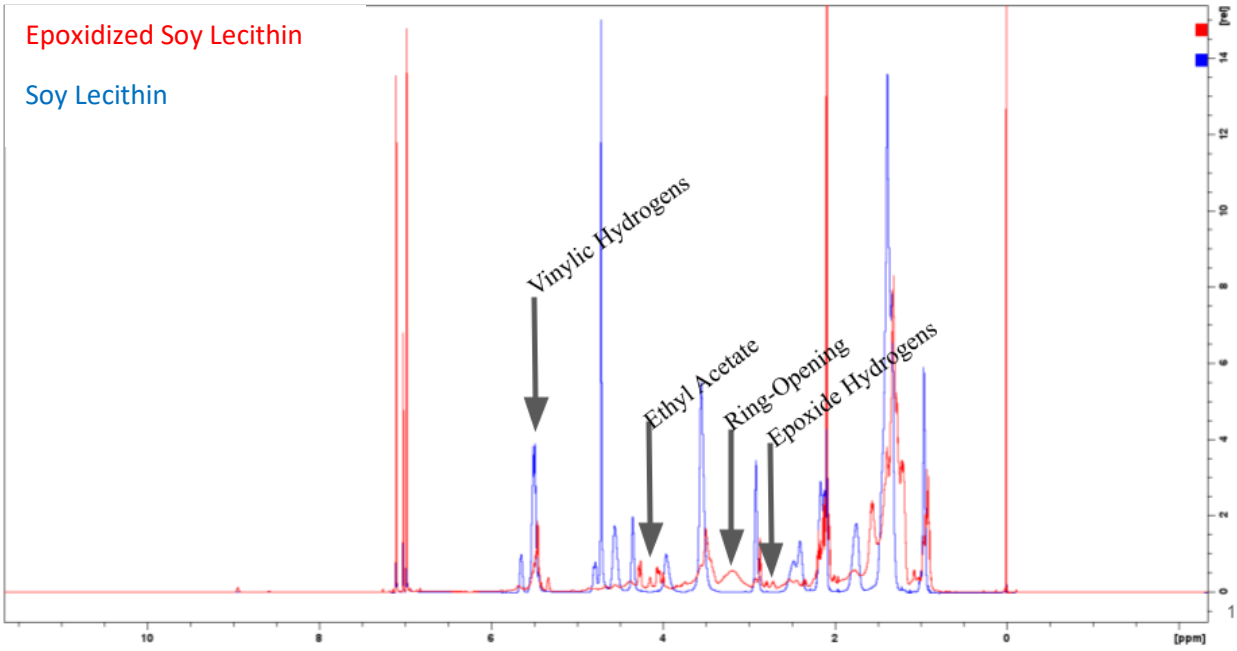

Figure 3.2. 1D ^{1}H NMR spectra of crude epoxidized soy lecithin and unreacted soy lecithin in in deuterated dimethyl sulfoxide (DMSO-d6)

The NMR spectra show the disappearance of the vinylic hydrogens ~5.5 ppm and a small epoxide hydrogen peak ~2.8 ppm. The NMR spectra also shows a broad new, broad peak in the aliphatic alcohol region (~3.2 ppm) which is evidence of the ring-opening of the newly formed epoxide groups. Isolated spectra of the regions of interest are available in the supporting

information (B.?). Because of this observation, subsequent epoxidation reactions were conducted at lower temperatures. The ring-opening occurs when the epoxide group continues to be oxidized by the peroxyformic acid in the solution. The epoxide group is preferred for the reaction with lignin as the strained ring conformation is more reactive. By lowering the temperature the over oxidation of the epoxide into the alcohol should be limited.

It should be noted that the NMR was taken of the crude product. Since the crude product had a high salt and acid content, the baseline of the NMR is not smooth. The decision not to purify the product was made to maintain atom economy and minimize the use of solvents in accordance with the principles of green chemistry[120].

The ESL and BCL linking reaction between was characterized via NMR (**Fig. 3.3**).

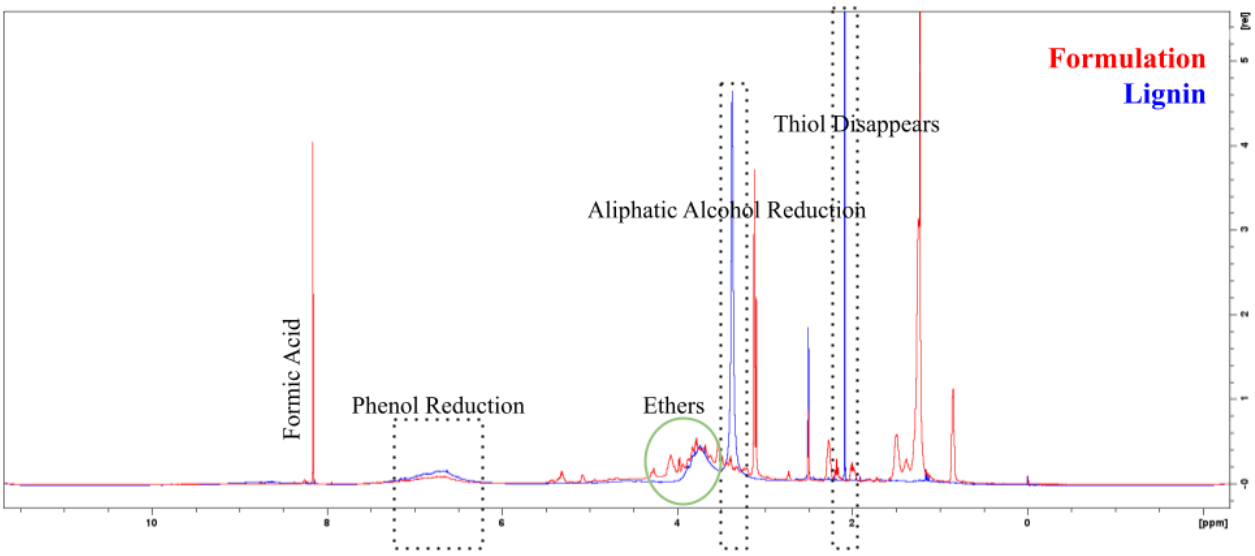

Figure 3.3. 1D ^{1}H NMR spectra of ESL and BCL formulation and BCL in DMSO-d6

It was originally hypothesized that the ESL would form ether linkages with the phenol groups within the BCL[68]. While the NMR did show some evidence of the reduction of phenolic functionality in the formulation there was a much more prominent reduction in the aliphatic

alcohol region (~3.2 ppm). Most notably the thiol peak from the BCL completely disappeared. This indicates that the epoxide groups likely reacted with the thiol groups within the BCL and forming sulfide linkages. This is particularly interesting from the application standpoint as the thiol group is in large part responsible for the distinctive odor of Kraft lignins[121]. The conversion of this group to a sulfide linkage may reduce the odor and make the formulation more desirable in food packaging or other applications in which an odor would be problematic.

3.3.2 Barrier Properties

The viability of the ESL+ BCL as a water barrier coating was first assessed by applying the coating to paperboard (**Table 3.1**). This formulation varies from the one used to coat the plastic films in that it does not contain the 2-butoxyethanol solvent. Instead, the formulation was applied to the paperboard immediately after removing it from the water bath so that it did not have time to cool and harden.

Table 3.1. Impact of ESL+L coating on the water barrier properties of paperboard

Material	**WVTR** **(g/(d*m^2))**	**WVP** **(g/(Pa*d*m))*10^{-6}**	**WCA** **(°)**	**Thickness** **(µm)**
Paperboard	3.55 ± 0.03	1.18 ± 0.01	58.72 ± 3.00	466 ± 2
ESL+L coated	1.6 ± 0.08	0.52 ± 0.02	20.59 ± 2.97	458 ± 5

Grammage of WestRock paperboard is 313 ± 2 g/m^2

The application of the coating to the paperboard significantly reduces the WVTR, WVP, and WCA by 55%, 56%, and 65% respectively. The reduction is WVTR and WVP is likely caused by a combination of added hydrophobic character and a reduction in porosity. The application also reduced the thickness of the paperboard. This could be caused by the pressure applied during coating collapsing the network or the coating causing adjacent fibers. The reduction in WCA is interesting in that the low contact angle indicates an increase in wettability of the surface. It is

possible that this reduction is caused by a decrease in surface roughness. On visual inspection, the lignin formulation was smooth and glossy both as a coating and as the cured coating alone. While this data cannot be directly compared to the coated plastic films, it does indicate that the combination of ESL and BCL can act as a barrier layer.

The coating as formulated above was too viscous to evenly coat the thin plastic films of ca. 20 μm thick. To remedy this 2-butoxyethanol was added as a solvent. The solubility of kraft lignin alone is complicated and the use of various organic solvents is frequently used to fractionate kraft lignins into more homogeneous fractions[122]. Traditional solvents like DMSO and acetone were able to solubilize the formulation, but are inappropriate for coating. 2-butoxyethanol has both polar and non-polar character. Its successful solvation of the ESL+L formulation is likely due to different fractions of lignin having affinities for either the polar or the nonpolar end of the solvent. The addition of 2-butoxyethanol resulted in a pourable formulation that could be developed at different formulation mass content. This formulation was used to coat the commercial plastic films that were then tested for water resistance (**table 3.2**).

Table 3.2. Impact of ESL+L coating on commercial plastic films.

Material	**WVTR** $(g/(d*m^2))$	**WVP** $(g/(Pa*d*m))*10^{-6}$	**WCA** (°)	**Thickness** (μm)
Commercial Film	71 ± 3	0.96 ± 0.04	67 ± 3	19 ± 1
Film + 10 w%	63 ± 3	1.33 ± 0.08	49 ± 3	29 ± 1
Film + 20 w%	59 ± 15	1.35 ± 0.34	26 ± 5	32 ± 1
Film + 50 w%	50 ± 4	1.28 ± 0.10	n/a	36 ± 1

The WVTR of the coated films decreased with increasing solids content. However when the thickness is accounted for as it is the case in the calculation of WVP the permeability increased by an average of 38% with the application of the coating, regardless of solids content. This may

indicate that the coating is mildly absorbent and traps water vapor within the structure as it diffuses through. This may be occurring at the polar (ionic) head group of the soy lecithin portion of the ESL+L formulation (**Fig. 3.5**). The water is likely able to hydrate the phosphatidylcholine zwitterion[123]. Like what was seen with the coated paperboard, the application of the coating decreased the contact angle. This could still be from a decrease in surface roughness, but given the corresponding increase in WVP, there is most likely some hydrophilic character at the surface. The ultimate application of this formulation will be coated onto a plastic film and then metalized, as the metal does not adhere well to the plastic itself. It is conjectured that the polar head group will coordinate with the aluminum ions and therefore not be able to interact with water potentially negating this issue.

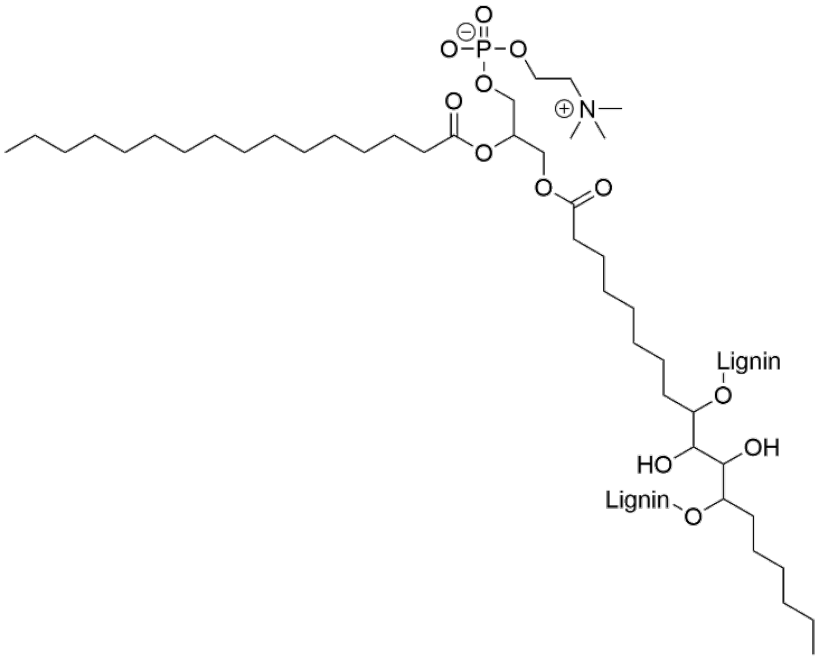

Figure 3.4. Hypothesized chemical structure of ESL+L formulation.

If the lignin is forming sulfide bonds as indicated by the NMR result, there are still free alcohol groups within the lignin that can interact with the water. However, kraft lignin on its own is water insoluble so interaction with these hydroxyl groups are likely minimal from the outset.

The coating formulation made of ESL and BCL alone demonstrated a highly brittle nature and tended to crack and flake off the coated plastic substrate. To address this issue 1 w% of unreacted soy lecithin was added as a plasticizer to increase the flexibility of the coating. The water resistance properties of these coating applied to the clear plastic films can be found in **table 3.3**.

Table 3.3. Impact of ESL+L with 1 w% plasticizer coating on commercial plastic films.

Material	WVTR ($g/(d*m^2)$)	WVP ($g/(Pa*d*m))*10^{-6}$	WCA (°)	Thickness (µm)
10 w% one coat	66.1 ± 3.3	1.05 ± 0.05	32 ± 5	22 ± 1
20 w% one coat	59.4 ± 1.4	1.14 ± 0.06	33 ± 5	27 ± 1
50 w% one coat	47.9 ± 1.7	1.31 ± 0.02	26 ± 5	38 ± 2

The 10 w% ESL+L that was applied had similar performance to the uncoated films. This very well may be due to how little coating was applied. When compared to the coatings without plasticizer the plasticized films have lower WVP, but it still increases with increasing solids content. This again is likely caused by small amounts of water trapped within the coating itself.

3.4 Summary

This preliminary work shows the potential of an ESL+L formulation to act as a bio-based barrier coating. The application of a single layer of formulation without plasticizer drastically lowers the water vapor permeability of the paperboard substrate, but this effect is less pronounced when coating the commercial plastic films. This is likely due to the already low permeability values of the uncoated films in combination with the limitations of the formulation itself and the inconsistency of lab-scale coating methods. The addition of 1 w% plasticizer lowered the water vapor permeability by an additional 10% indicating that flaws within the coating are likely artificially increasing the measured permeability. Suggestions for further work can be found in **Chapter 4**.

CHAPTER 4: Summary and Future Work

4.1 Chapter 1

The motivation for this work was to investigate possible solutions to the plastic waste crisis with the goal of finding a sustainable alternative to multilayer packaging components. To achieve this goal five different biopolymers, (bacterial nanocellulose, alginate, zein, lignin, and soy lecithin) were combined to form composite films and coatings for water barrier applications.

This chapter also provides background information on the scale of the plastic waste problem and on how the packing industry is responsible for nearly half of all plastic waste produced. The benefits and drawbacks of multilayer packaging were covered to emphasize the need for a sustainable solution. A brief history of biopolymer packaging was provided before delving into current biocomposite film and coating research. Lastly, details on the five chosen biopolymers was given.

4.2 Chapter 2

Chapter 2 detailed the development of ternary biocomposite films of bacterial nanocellulose, alginate and zein. Two-component systems of bacterial nanocellulose with either alginate or zein were carefully studied with and without the addition of divalent calcium ions and an ionic crosslinking agent. The mass ratio of the three components in the ternary films were determined from the best performing two component films. Using mechanical performance and water barrier data in conjunction with SEM and XPS cohesive models of arrangement for both the crosslinked and uncrosslinked films were developed.

Both models depict an interpenetrating network of bacterial nanocellulose and alginate. Without the presence of the crosslinker the zein adheres to the surface of the cellulose via ion-dipole interactions between carboxylate ions within the zein and polar groups on the cellulose fibril surfaces. When the ionic crosslinker is added the g-blocks of alginate coordinate with the ion

according to the egg-box model reinforcing the interpenetrating bacterial nanocellulose network. The zein reacts to the presence of the calcium ions similarly, forming spherical aggregates within and at the surface of the films. This detailed knowledge of the method of assembly within the films could allow for the strategic development of a high-performance film for use in food packaging.

4.3 Chapter 3

Chapter 3 covers the preliminary work done on developing a lignin-based barrier coating for commercial plastic films. Soy lecithin was epoxidized at the unsaturated C=C bonds in the fatty acid tails. These highly strained epoxy groups were then reacted with unwashed BioChoice kraft lignin resulting in ester and sulfide bonds between the lecithin and lignin. This coating was applied to paperboard to confirm its ability to lower water vapor permeability. The viscosity of the coating was modified with 2-butoxyethanol resulting in a formulation of appropriate for bar coating.

The influence of the solids content of the coating slurry as well as the presence of a plasticizer on both water vapor permeability and water contact angle were measured. The results were mixed. The coating resulted in a large drop in permeability for the paperboard, but this was not shown for the commercial plastic films. Since the permeability of the plastic films is already very low the small amount of water absorbed into the coating itself was detectable.

4.4 Suggestions for Future Study

Both the bacterial nanocellulose films project and the lignin coating project show potential for further study and application. Suggestions for each project are found below.

The distribution and conformation of zein within the films deserves further study, particularly zein's aggregation behavior in the presence of calcium ions. Surface roughness should be analyzed via atomic force microscopy. This in combination with elemental mapping via EDS

for nitrogen would allow for confirmation that the addition of zein increases the surface roughness of the films and that the zein was evenly distributed throughout as micro-scale aggregates. A zeta potential experiment may also be able to give information about zein's behavior in the presence of calcium ions. The zein shows a negative zeta potential due to the exposed carboxylate ions from the deamidation reaction. If the zein aggregates around the calcium ions by forming ionic bonds with the carboxylate ions the zeta potential should move in the positive direction with the addition of calcium to a zein solution.

Alternative solvents should also be considered for the bacterial nanocellulose films. Zein is soluble in aqueous alcohol solutions without undergoing a deamidation reaction, preserving the surface hydrophobicity of the zein protein. However, alginate is not soluble in alcohol. Different solvent conditions including aqueous alcohols and 2-butoxyethanol may be able to dissolve both the zein and alginate allowing for the study of the system with zein in a different conformation.

The bacterial cellulose obtained from *nata de coco* needs to be characterized to determine size distribution and aspect ratio. It may be possible to determine the scale of the bacterial cellulose via XRD. Determining the crystallinity before and after homogenization with the aqueous counter collision system would be worthwhile, as others have reported a change in crystal conformation of bacterial cellulose after ACC[124].

The preliminary work done with the lignin-based coatings should be continued, and the coating formulation should be further optimized. A second layer of coating should be applied to obscure the flaws in the first layer which may result in a lower water vapor permeability even with the increased thickness. Large plasticizer content along with other plasticizers should also be considered to reduce the brittleness of the lignin and create a coating with fewer flaws that artificially inflate the measured water vapor permeability. TGA experiments should be conducted

on the coating formulation before and after conditioning at TAPPI standard conditions the water content. The lignin-based coating should also be applied to cellulosic surfaces, potentially including nanocellulose films, to show its water barrier properties in an environment with higher tolerance for defects.

Outside of using the lignin-ESL formulation for coating, it is possible that with enough plasticizer self-standing films could be formed. Testing the water barrier properties of these films would likely show a very low water vapor permeability on the scale of commercial PLA. Given the thermoplastic nature of lignin, these may be able to be extruded for use in multilayer packaging on its own.

REFERENCES

1. United Nations. The future we want. (2012).

2. G7 Summit. Leader's Declaration. (2015).

3. Naidoo, M. & Gasparatos, A. Corporate environmental sustainability in the retail sector: Drivers, strategies and performance measurement. *Journal of Cleaner Production* **203**, 125–142 (2018).

4. Basel Convention. Basel Convention Waste Ammendments. http://www.basel.int/Implementation/Plasticwaste/Amendments/Overview/tabid/8426/Default.aspx (2019).

5. United Nations Environment Programme. *Neglected: Environmental Justice Impacts of Marine Litter and Plastic Pollution*. (2021).

6. Geyer, R., Jambeck, J. R. & Law, K. L. Production, use, and fate of all plastics ever made. *Science Advances* **3**, (2017).

7. Environmental Protection Agency, U., of Land, O., Management, E. & of Resource Conservation, O. *Advancing Sustainable Materials Management: 2018 Tables and Figures Assessing Trends in Materials Generation and Management in the United States*. (2018).

8. Han, J.-W., Ruiz-Garcia, L., Qian, J.-P. & Yang, X.-T. Food Packaging: A Comprehensive Review and Future Trends. *Comprehensive Reviews in Food Science and Food Safety* **17**, 860–877 (2018).

9. Jog, J. P. Crystallization of Polyethyleneterephthalate. *https://doi.org/10.1080/15321799508014598* **35**, 531–553 (1995).

10. Bekhta, P., Lyutyy, P., Hiziroglu, S. & Ortynska, G. Properties of Composite Panels Made from Tetra-Pak and Polyethylene Waste Material. *Journal of Polymers and the Environment* **24**, 159–165 (2016).

11. Horodytska, O., Valdés, F. J. & Fullana, A. Plastic flexible films waste management – A state of art review. *Waste Management* **77**, 413–425 (2018).

12. Alex Tullo. Industry's plastics recycling bet. *C&EN Global Enterprise* **98**, 27–32 (2020).

13. Choudhary, A., Chatterjee, S. & Prasad, E. Biodegradable Plastic Market Size, Share | Industry Forecast, 2027. *MC: Advanced Materials* https://www.alliedmarketresearch.com/biodegradable-plastic-market (2020).

14. Taib, N. A. A. B. *et al.* A review on poly lactic acid (PLA) as a biodegradable polymer. *Polymer Bulletin* 1–35 (2022) doi:10.1007/S00289-022-04160-Y/TABLES/14.

15. Huang, D. *et al.* Seawater degradation of PLA accelerated by water-soluble PVA. *E-Polymers* **20**, 759–772 (2020).

16. Risch, S. J. Food Packaging History and Innovations. *Journal of Agricultural and Food Chemistry* **57**, 8089–8092 (2009).

17. Krupp, L. R. & Jewell, W. J. Biodegradability of Modified Plastic Films in Controlled Biological Environments. *Environmental Science and Technology* **26**, 193–198 (1992).

18. Imam, S. H. *et al.* Fate of starch-containing plastic films exposed in aquatic habitats. *Current Microbiology 1992 25:1* **25**, 1–8 (1992).

19. Whitney, P. J., Swaffield, C. H. & Graffham, A. J. The environmental degradation of thin plastic films. *International Biodeterioration and Biodegradation* **31**, 179–198 (1993).

20. Science to Enable Sustainable Plastics. in *8th Chemical Sciences and Society Summit* (2020).

21. Klemm, D. *et al.* Nanocelluloses: A New Family of Nature-Based Materials. *Angewandte Chemie International Edition* **50**, 5438–5466 (2011).

22. Ferrer, A., Pal, L. & Hubbe, Martin. Nanocellulose in packaging: Advances in barrier layer technologies. *Industrial Crops and Products* **95**, 574–582 (2017).

23. FDA's Approach to the GRAS Provision: A History of Processes | FDA. https://www.fda.gov/food/generally-recognized-safe-gras/fdas-approach-gras-provision-history-processes.

24. Cazón, P. & Vázquez, M. Bacterial cellulose as a biodegradable food packaging material: A review. *Food Hydrocolloids* **113**, 106530 (2021).

25. Reiniati, I., Hrymak, A. N. & Margaritis, A. Recent developments in the production and applications of bacterial cellulose fibers and nanocrystals. *Critical Reviews in Biotechnology* **37**, 510–524 (2017).

26. Pecoraro, E., Manzani, D., Messaddeq, Y. & Ribeiro, S. J. L. Bacterial Cellulose from Glucanacetobacter xylinus: Preparation, Properties and Applications. in *Monomers, polymers and composites from renewable resources* (eds. Belgacem, M. N. & Gandini, A.) 369–383 (Elsevier Science & Technology, 2008).

27. Park, J. K., Jung, J. Y. & Khan, T. 26 - Bacterial cellulose. in *Handbook of Hydrocolloids (Second Edition)* (eds. Phillips, G. O. & Williams, P. A.) 724–739 (Woodhead Publishing, 2009).

28. Iguchi, M., Yamanaka, S. & Budhiono, A. Review Bacterial cellulose-a masterpiece of nature's arts. *Journal of materials science* **35**, 261–270 (2000).

29. Kwak, M. H. *et al.* Bacterial cellulose membrane produced by Acetobacter sp. A10 for burn wound dressing applications. *Carbohydrate Polymers* **122**, 387–398 (2015).

30. Provin, A. P. *et al.* Use of bacterial cellulose in the textile industry and the wettability challenge - a review. *Cellulose* **28**, 8255–8274 (2021).

31. Barud, H. S. *et al.* Bacterial cellulose/poly(3-hydroxybutyrate) composite membranes. *Carbohydrate Polymers* **83**, 1279–1284 (2011).

32. Mihaela Jipa, I. *et al.* Preparation and characterization of bacterial cellulose-poly(vinyl alcohol) films with antimicrobial properties. *Materials Letters* **66**, 125–127 (2012).

33. Martínez-Sanz, M., Olsson, R. T., Lopez-Rubio, A. & Lagaron, J. M. Development of bacterial cellulose nanowhiskers reinforced EVOH composites by electrospinning. *Journal of Applied Polymer Science* **124**, 1398–1408 (2012).

34. Wang, X. *et al.* Physical properties and antioxidant capacity of chitosan/epigallocatechin-3-gallate films reinforced with nano-bacterial cellulose. *Carbohydrate Polymers* **179**, 207–220 (2018).

35. Woehl, M. A. *et al.* Bionanocomposites of thermoplastic starch reinforced with bacterial cellulose nanofibres: Effect of enzymatic treatment on mechanical properties. *Carbohydrate Polymers* **80**, 866–873 (2010).

36. Chiaoprakobkij, N., Seetabhawang, S., Sanchavanakit, N. & Phisalaphong, M. Fabrication and characterization of novel bacterial cellulose/alginate/gelatin biocomposite film. *Journal of Biomaterials Science, Polymer Edition* **30**, 961–982 (2019).

37. Feng, Y., Zhang, X., Shen, Y., Yoshino, K. & Feng, W. A mechanically strong, flexible and conductive film based on bacterial cellulose/graphene nanocomposite. *Carbohydrate Polymers* **87**, 644–649 (2012).

38. Vu, C. M. *et al.* Environmentally benign green composites based on epoxy resin/bacterial cellulose reinforced glass fiber: Fabrication and mechanical characteristics. *Polymer Testing* **61**, 150–161 (2017).

39. Rahman, K. U. *et al.* Flexible bacterial cellulose-based BC-SiO2-TiO2-Ag membranes with self-cleaning, photocatalytic, antibacterial and UV-shielding properties as a potential multifunctional material for combating infections and environmental applications. *Journal of Environmental Chemical Engineering* **9**, 104708 (2021).

40. Collins, M. N. *et al.* Valorization of lignin in polymer and composite systems for advanced engineering applications – A review. *International Journal of Biological Macromolecules* **131**, 828–849 (2019).

41. Crestini, C., Lange, H., Sette, M. & Argyropoulos, D. S. On the structure of softwood kraft lignin. *Green Chemistry* **19**, 4104–4121 (2017).

42. Norgren, M. & Edlund, H. Lignin: Recent advances and emerging applications. *Current Opinion in Colloid and Interface Science* **19**, 409–416 (2014).

43. Liao, J. J., Latif, N. H. A., Trache, D., Brosse, N. & Hussin, M. H. Current advancement on the isolation, characterization and application of lignin. *International Journal of Biological Macromolecules* **162**, 985–1024 (2020).

44. Saibuatong, O. ard & Phisalaphong, M. Novo aloe vera–bacterial cellulose composite film from biosynthesis. *Carbohydrate Polymers* **79**, 455–460 (2010).

45. Phisalaphong, M. & Jatupaiboon, N. Biosynthesis and characterization of bacteria cellulose–chitosan film. *Carbohydrate Polymers* **74**, 482–488 (2008).

46. Yang, Y.-N. *et al.* Development of bacterial cellulose/chitin multi-nanofibers based smart films containing natural active microspheres and nanoparticles formed in situ. *Carbohydrate polymers* **228**, 115370 (2020).

47. Cheng, K. C., Catchmark, J. M. & Demirci, A. Effect of different additives on bacterial cellulose production by Acetobacter xylinum and analysis of material property. *Cellulose* **16**, 1033–1045 (2009).

48. Kanjanamosit, N., Muangnapoh, C. & Phisalaphong, M. Biosynthesis and characterization of bacteria cellulose–alginate film. *Journal of Applied Polymer Science* **115**, 1581–1588 (2010).

49. Cielecka, I. *et al.* Glycerol-plasticized bacterial nanocellulose-based composites with enhanced flexibility and liquid sorption capacity. *Cellulose* **26**, 5409–5426 (2019).

50. Ma, X. *et al.* In situ formed active and intelligent bacterial cellulose/cotton fiber composite containing curcumin. *Cellulose* **27**, 9371–9382 (2020).

51. Ul-Islam, M., Shah, N., Ha, J. H. & Park, J. K. Effect of chitosan penetration on physico-chemical and mechanical properties of bacterial cellulose. *Korean Journal of Chemical Engineering 2011 28:8* **28**, 1736–1743 (2011).

52. Vázquez, M., Velazquez, G. & Cazón, P. UV-Shielding films of bacterial cellulose with glycerol and chitosan. Part 2: Structure, water vapor permeability, spectral and thermal properties. *http://mc.manuscriptcentral.com/tcyt* **19**, 115–126 (2021).

53. Li, G. *et al.* An environmentally benign approach to achieving vectorial alignment and high microporosity in bacterial cellulose/chitosan scaffolds. *RSC Advances* **7**, 13678–13688 (2017).

54. Lin, S. Bin, Hsu, C. P., Chen, L. C. & Chen, H. H. Adding enzymatically modified gelatin to enhance the rehydration abilities and mechanical properties of bacterial cellulose. *Food Hydrocolloids* **23**, 2195–2203 (2009).

55. Yang, G., Yao, Y. & Wang, C. Green synthesis of silver nanoparticles impregnated bacterial cellulose-alginate composite film with improved properties. *Materials Letters* **209**, 11–14 (2017).

56. Yang, J.-S., Xie, Y.-J. & He, W. Research progress on chemical modification of alginate: A review. *Carbohydrate Polymers* **84**, 33–39 (2011).

57. Sirviö, J. A., Kolehmainen, A., Liimatainen, H., Niinimäki, J. & Hormi, O. E. O. Biocomposite cellulose-alginate films: Promising packaging materials. *Food Chemistry* **151**, 343–351 (2014).

58. Naseri, N., Deepa, B., Mathew, A. P., Oksman, K. & Girandon, L. Nanocellulose-Based Interpenetrating Polymer Network (IPN) Hydrogels for Cartilage Applications. *Biomacromolecules* **17**, 3714–3723 (2016).

59. Lima, H. L. S. *et al.* Bacterial cellulose nanofiber-based films incorporating gelatin hydrolysate from tilapia skin: production, characterization and cytotoxicity assessment. *Cellulose* **25**, 6011–6029 (2018).

60. Wan, Z., Wang, L., Ma, L., Sun, Y. & Yang, X. Controlled Hydrophobic Biosurface of Bacterial Cellulose Nanofibers through Self-Assembly of Natural Zein Protein. *ACS Biomaterials Science and Engineering* **3**, 1595–1604 (2017).

61. Viana, R. M., Sá, N. M. S. M. S. M., Barros, M. O., Borges, M. de F. & Azeredo, H. M. C. C. Nanofibrillated bacterial cellulose and pectin edible films added with fruit purees. *Carbohydrate polymers* **196**, 27–32 (2018).

62. Oliveira-Alcântara, A. V. *et al.* Bacterial cellulose/cashew gum films as probiotic carriers. *Lwt* **130**, 109699 (2020).

63. Atta, O. M. *et al.* Development and characterization of yeast-incorporated antimicrobial cellulose biofilms for edible food packaging application. *Polymers* **13**, 2310 (2021).

64. Cruz, T. M. *et al.* Hybrid films from plant and bacterial nanocellulose: mechanical and barrier properties. *Nordic Pulp and Paper Research Journal* **37**, 159–174 (2022).

65. Nascimento, E. S. *et al.* All-cellulose nanocomposite films based on bacterial cellulose nanofibrils and nanocrystals. *Food Packaging and Shelf Life* **29**, (2021).

66. Wen, Y. *et al.* Development of intelligent/active food packaging film based on TEMPO-oxidized bacterial cellulose containing thymol and anthocyanin-rich purple potato extract for shelf life extension of shrimp. *Food Packaging and Shelf Life* **29**, 100709 (2021).

67. Khan, T. A., Lee, J.-H. & Kim, H.-J. Lignin-Based Adhesives and Coatings. in *Lignocellulose for Future Bioeconomy* 153–206 (2019).

68. Hult, E. L. *et al.* Esterified lignin coating as water vapor and oxygen barrier for fiber-based packaging. *Holzforschung* **67**, 899–905 (2013).

69. Hult, E. L., Ropponen, J., Poppius-Levlin, K., Ohra-Aho, T. & Tamminen, T. Enhancing the barrier properties of paper board by a novel lignin coating. *Industrial Crops and Products* **50**, 694–700 (2013).

70. Antonsson, S., Henriksson, G., Johansson, M. & Lindström, M. E. Low Mw-lignin fractions together with vegetable oils as available oligomers for novel paper-coating applications as hydrophobic barrier. *Industrial Crops and Products* **27**, 98–103 (2008).

71. Shukla, R. & Cheryan, M. Zein: the industrial protein from corn. *Industrial Crops and Products* **13**, 171–192 (2001).

72. Giteru, S. G., Ali, M. A. & Oey, I. Recent progress in understanding fundamental interactions and applications of zein. *Food Hydrocolloids* **120**, 106948 (2021).

73. Wang, Y. & Padua, G. W. Formation of zein spheres by evaporation-induced self-assembly. *Colloid and Polymer Science* **290**, 1593–1598 (2012).

74. Yin, B., Wang, C., Liu, Z. & Yao, P. Peptide-polysaccharide conjugates with adjustable hydrophilicity/hydrophobicity as green and pH sensitive emulsifiers. *Food Hydrocolloids* **63**, 120–129 (2017).

75. Grant, G. T., Morris, E. R., Rees, D. A., Smith, P. J. C. & Thom, D. Biological interactions between polysaccharides and divalent cations: The egg-box model. *FEBS Letters* **32**, 195–198 (1973).

76. Donati, I. *et al.* New Hypothesis on the Role of Alternating Sequences in Calcium−Alginate Gels. *Biomacromolecules* **6**, 1031–1040 (2005).

77. Li, L., Fang, Y., Vreeker, R., Appelqvist, I. & Mendes, E. Reexamining the Egg-Box Model in Calcium−Alginate Gels with X-ray Diffraction. *Biomacromolecules* **8**, 464–468 (2007).

78. Scholfield, C. R. Composition of soybean lecithin. *Journal of the American Oil Chemists' Society* **58**, 889–892 (1981).

79. List, G. R. Soybean Lecithin: Food, Industrial Uses, and Other Applications. *Polar Lipids: Biology, Chemistry, and Technology* 1–33 (2015) doi:10.1016/B978-1-63067-044-3.50005-4.

80. Deffense, E. Chemical Degumming. *The American Oil Chemists' Society* https://lipidlibrary.aocs.org/edible-oil-processing/chemical-degumming.

81. Hilditch, T. P. & Zaky, Y. A. H. The component fatty acids of some vegetable seed phosphatides. *Biochemical Journal* **36**, 815 (1942).

82. Vijayalakshmi, B. & Rao, S. V. Fatty acid composition of phospholipids in seed oils containing unusual acids. *Chemistry and Physics of Lipids* **9**, 82–86 (1972).

83. Jin, J. *et al.* An efficient and environmental-friendly dispersant based on the synergy of amphiphilic surfactants for oil spill remediation. *Chemosphere* **215**, 241–247 (2019).

84. Nyankson, E., Olasehinde, O., John, V. T. & Gupta, R. B. Surfactant-Loaded Halloysite Clay Nanotube Dispersants for Crude Oil Spill Remediation. *Industrial and Engineering Chemistry Research* **54**, 9328–9341 (2015).

85. Nyankson, E., Demir, M., Gonen, M. & Gupta, R. B. Interfacially Active Hydroxylated Soybean Lecithin Dispersant for Crude Oil Spill Remediation. *ACS Sustainable Chemistry and Engineering* **4**, 2056–2067 (2016).

86. Nkanga, C. I., Krause, R. W., Noundou, X. S. & Walker, R. B. Preparation and characterization of isoniazid-loaded crude soybean lecithin liposomes. *International Journal of Pharmaceutics* **526**, 466–473 (2017).

87. Mahjour, M., Mauser, B., Rashidbaigi, Z. & Fawzi, M. B. Effect of egg yolk lecithins and commercial soybean lecithins on in vitro skin permeation of drugs. *Journal of Controlled Release* **14**, 243–252 (1990).

88. Stoltz, J. F. *et al.* Effect of soybean-lecithin as an enhancer of buccal mucosa absorption of insulin. *Bio-Medical Materials & Engineering* **22**, 171–178 (2012).

89. Zhang, S.-S., Hu, J.-H., Li, Q.-W., Jiang, Z.-L. & Zhang, X.-Y. The cryoprotective effects of soybean lecithin on boar spermatozoa quality. *African Journal of Biotechnology* **8**, 6476–6480 (2009).

90. Papa, F. O. *et al.* Replacing egg yolk with soybean lecithin in the cryopreservation of stallion semen. *Animal Reproduction Science* **129**, 73–77 (2011).

91. Salmani, H., Towhidi, A., Zhandi, M., Bahreini, M. & Sharafi, M. In vitro assessment of soybean lecithin and egg yolk based diluents for cryopreservation of goat semen. *Cryobiology* **68**, 276–280 (2014).

92. Zhong, C. Industrial-Scale Production and Applications of Bacterial Cellulose. *Frontiers in Bioengineering and Biotechnology* **8**, 1425 (2020).

93. Li, Q. *et al.* Nanocomposites of Bacterial Cellulose Nanofibrils and Zein Nanoparticles for Food Packaging. *ACS Applied Nano Materials* **3**, 2899–2910 (2020).

94. Ju, S., Zhang, F., Duan, J. & Jiang, Jianxin. Characterization of bacterial cellulose composite films incorporated with bulk chitosan and chitosan nanoparticles: A comparative study. *Carbohydrate Polymers* **237**, 116167 (2020).

95. Lee, K. Y. & Mooney, D. J. Alginate: Properties and biomedical applications. *Progress in Polymer Science* **37**, 106–126 (2012).

96. Hernández-Carmona, G., McHugh, D. J., Arvizu-Higuera, D. L. & Rodríguez-Montesinos, Y. E. Pilot plant scale extraction of alginates from Macrocystis pyrifera 4. Conversion of alginic acid to sodium alginate, drying and milling. *Journal of Applied Phycology* **14**, 445–451 (2002).

97. Benselfelt, T., Engström, J. & Wågberg, L. Supramolecular double networks of cellulose nanofibrils and algal polysaccharides with excellent wet mechanical properties. *Green Chemistry* **20**, 2558–2570 (2018).

98. Goldstein, J. I. *et al.* Coating Techniques for SEM and Microanalysis. in *Scanning Electron Microscopy and X-Ray Microanalysis* 461–494 (Springer, Boston, MA, 1981). doi:10.1007/978-1-4613-3273-2_10.

99. Zhang, B., Luo, Y. & Wang, Q. Effect of acid and base treatments on structural, rheological, and antioxidant properties of α-zein. *Food Chemistry* **124**, 210–220 (2011).

100. Sun, J. Y. *et al.* Highly stretchable and tough hydrogels. *Nature* **489**, 133–136 (2012).

101. Sun, C., Chen, S., Dai, L. & Gao, Y. Structural characterization and formation mechanism of zein-propylene glycol alginate binary complex induced by calcium ions. *Food Research International* **100**, 57–68 (2017).

102. Cabra, V., Arreguin, R., Vazquez-Duhalt, R. & Farres, A. Effect of Alkaline Deamidation on the Structure, Surface Hydrophobicity, and Emulsifying Properties of the Z19 α-Zein. *Journal of Agricultural and Food Chemistry* **55**, 439–445 (2006).

103. Chen, H. & Zhong, Q. A novel method of preparing stable zein nanoparticle dispersions for encapsulation of peppermint oil. *Food Hydrocolloids* **43**, 593–602 (2015).

104. Abdollahi, M., Alboofetileh, M., Behrooz, R., Rezaei, M. & Miraki, R. Reducing water sensitivity of alginate bio-nanocomposite film using cellulose nanoparticles. *International Journal of Biological Macromolecules* **54**, 166–173 (2013).

105. Ummartyotin, S., Pisitsak, P. & Pechyen, C. Eggshell and Bacterial Cellulose Composite Membrane as Absorbent Material in Active Packaging. *International journal of polymer science* **2016**, 1–8 (2016).

106. Kulasinski, K., Guyer, R., Derome, D. & Carmeliet, J. Water Diffusion in Amorphous Hydrophilic Systems: A Stop and Go Process. *Langmuir* **31**, 10843–10849 (2015).

107. Fox, R. Aseptic packaging materials and sterilants. in *Handbook of aseptic processing and packaging* 103–118 (Taylor & Francis Group, 2012).

108. Abral, H. *et al.* A simple strategy in enhancing moisture and thermal resistance and tensile properties of disintegrated bacterial cellulose nanopaper. *Journal of Materials Research and Technology* **9**, 8754–8765 (2020).

109. Lichtenstein, K. & Lavoine, N. Toward a deeper understanding of the thermal degradation mechanism of nanocellulose. *Polymer Degradation and Stability* **146**, 53–60 (2017).

110. Nurazzi, N. M. *et al.* Thermogravimetric analysis properties of cellulosic natural fiber polymer composites: A review on influence of chemical treatments. *Polymers* **13**, (2021).

111. Trossaert, L., De Vel, M., Cardon, L. & Edeleva, M. Lifting the Sustainability of Modified Pet-Based Multilayer Packaging Material with Enhanced Mechanical Recycling Potential and Processing. *Polymers* **14**, (2022).

112. Hossain, R., Al Mahmood, A. & Sahajwalla, V. Facile Solution for Recycling Hazardous Flexible Plastic-Laminated Metal Packaging Waste to Produce Value-Added Metal Alloys. *ACS Sustainable Chemistry and Engineering* **9**, 16881–16895 (2021).

113. Bauer, A. S. *et al.* Recyclability and redesign challenges in multilayer flexible food packaging—a review. *Foods* **10**, (2021).

114. Laurichesse, S. & Avérous, L. Chemical modification of lignins: Towards biobased polymers. *Progress in Polymer Science* **39**, 1266–1290 (2014).

115. Yang, W. *et al.* Antioxidant and antibacterial lignin nanoparticles in polyvinyl alcohol/chitosan films for active packaging. *Industrial Crops and Products* **94**, 800–811 (2016).

116. Aguié-Béghin, V. *et al.* Use of Food and Packaging Model Matrices to Investigate the Antioxidant Properties of Biorefinery Grass Lignins. *Journal of Agricultural and Food Chemistry* **63**, 10022–10031 (2015).

117. Domenek, S., Louaifi, A., Guinault, A. & Baumberger, S. Potential of Lignins as Antioxidant Additive in Active Biodegradable Packaging Materials. *Journal of Polymers and the Environment* **21**, 692–701 (2013).

118. Wang, C., Kelley, S. S. & Venditti, R. A. Lignin-Based Thermoplastic Materials. *ChemSusChem* **9**, 770–783 (2016).

119. Barcena, H., Tuachi, A. & Zhang, Y. Teaching Green Chemistry with Epoxidized Soybean Oil. *Journal of Chemical Education* **94**, 1314–1318 (2017).

120. 12 Principles of Green Chemistry - American Chemical Society. https://www.acs.org/content/acs/en/greenchemistry/principles/12-principles-of-green-chemistry.html.

121. Lok, B. *et al.* Odor and Constituent Odorants of HDPE–Lignin Blends of Different Lignin Origin. *Polymers* **14**, 1–22 (2022).

122. Duval, A., Vilaplana, F., Crestini, C. & Lawoko, M. Solvent screening for the fractionation of industrial kraft lignin. *Holzforschung* **70**, 11–20 (2016).

123. Lundberg, B., Svens, E. & Ekman, S. The hydration of phospholipids and phospholipid-cholesterol complexes. *Chemistry and physics of lipids* **22**, 285–292 (1978).

124. Tatsumi, D., Kanda, A. & Kondo, T. Characterization of mercerized cellulose nanofibrils prepared by aqueous counter collision process. *Journal of Wood Science* **68**, 1–9 (2022).

125. L-a-Lecithin, Soybean - CAS 8002-43-5 - Calbiochem L-a-Lecithin, Soybean, CAS 8002-43-5, is a concentrate of soybean lecithin consisting of more than 94 phosphatidylcholine and less than 2 triglycerides. 8002-43-5. https://www.sigmaaldrich.com/US/en/product/mm/429415.

126. Hu, Z., Du, X., Liu, J., Chang, H. M. & Jameel, H. Structural Characterization of Pine Kraft Lignin: BioChoice Lignin vs Indulin AT. *Journal of Wood Chemistry and Technology* **36**, 432–446 (2016).

APPENDICES

Appendix A – Supporting Information Chapter 2

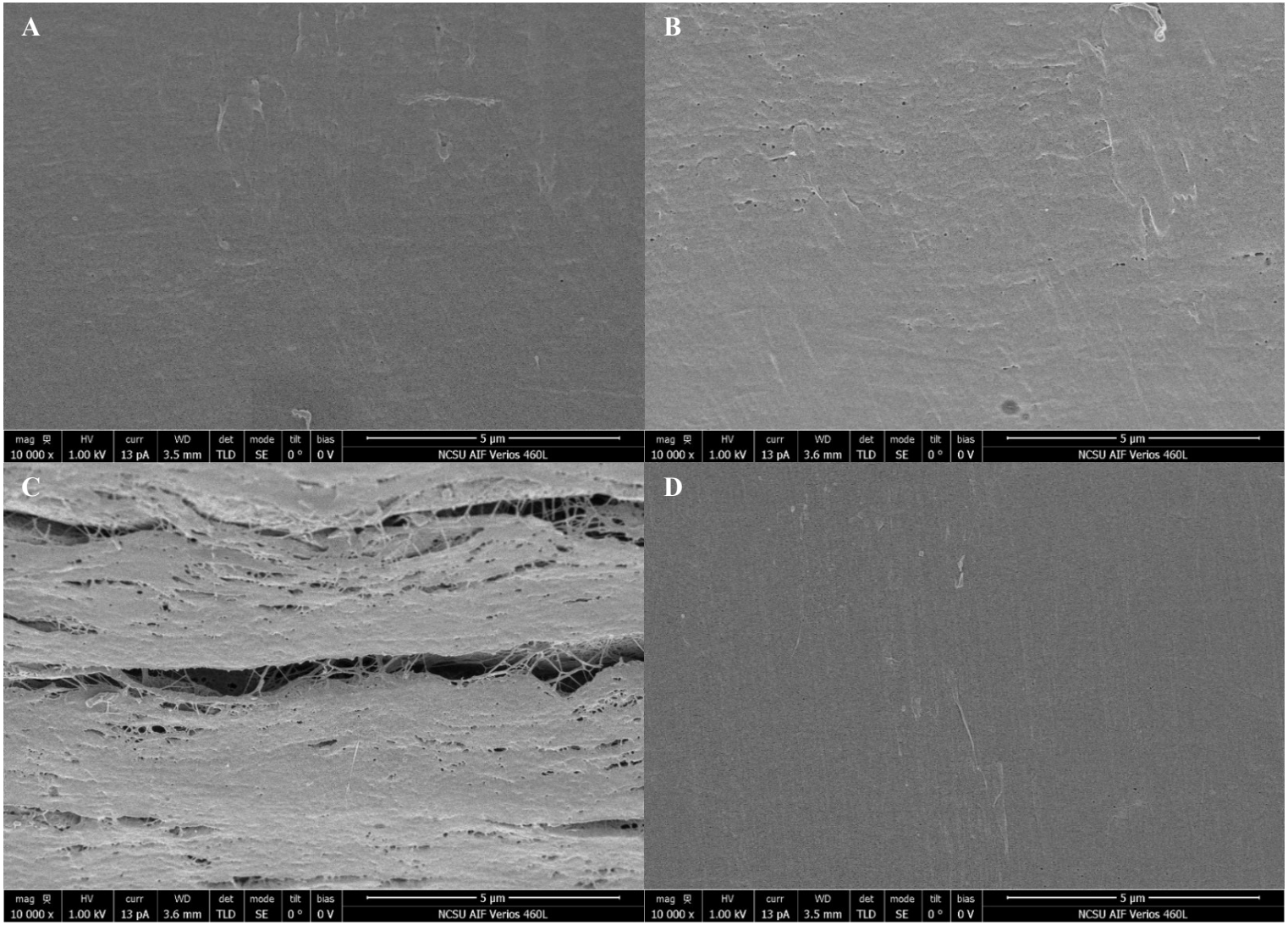

Figure A1. SEM images of film cross sections at 10000x magnification. (A) BC, (B) 90:10 BC/Z, (C) 70:30 BC/A, (D) 60:30:10 BC/A/Z

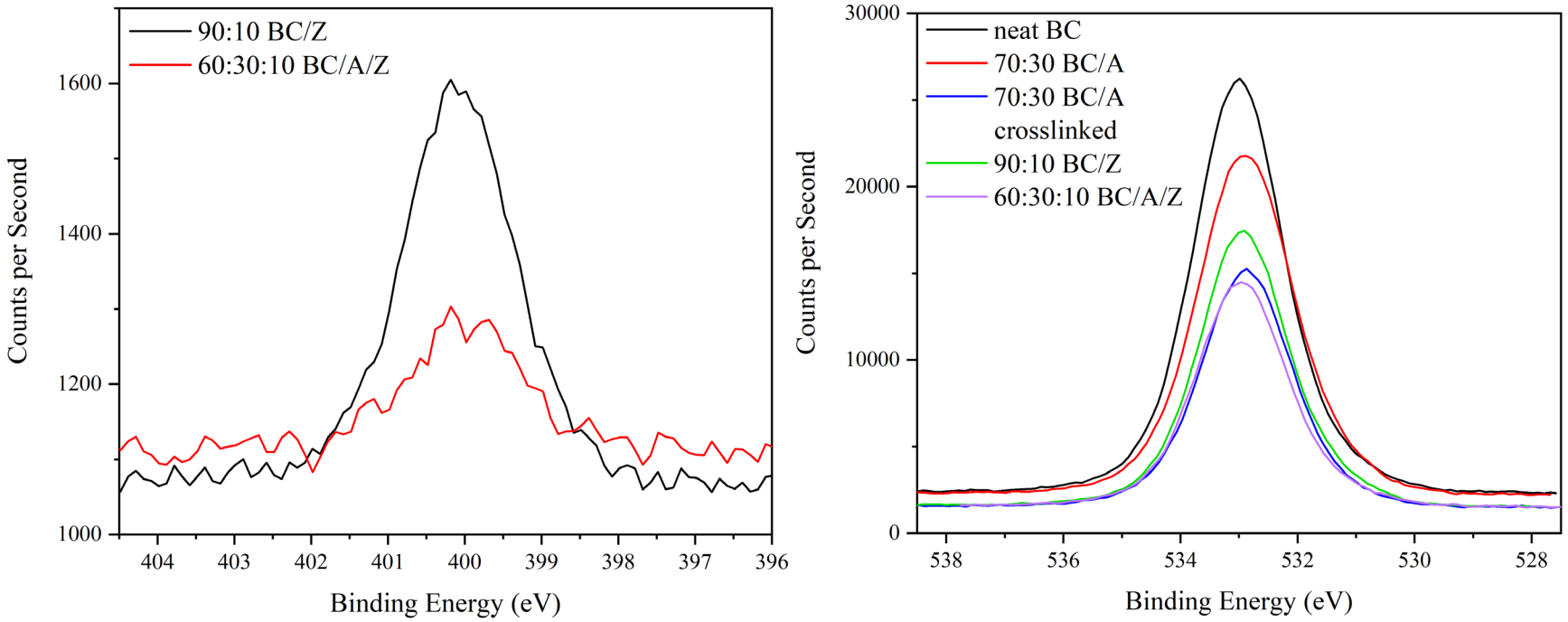

Figure A2. (A) High resolution XPS nitrogen scan and (B) high resolution XPS oxygen scan of vacuum filtered film surfaces.

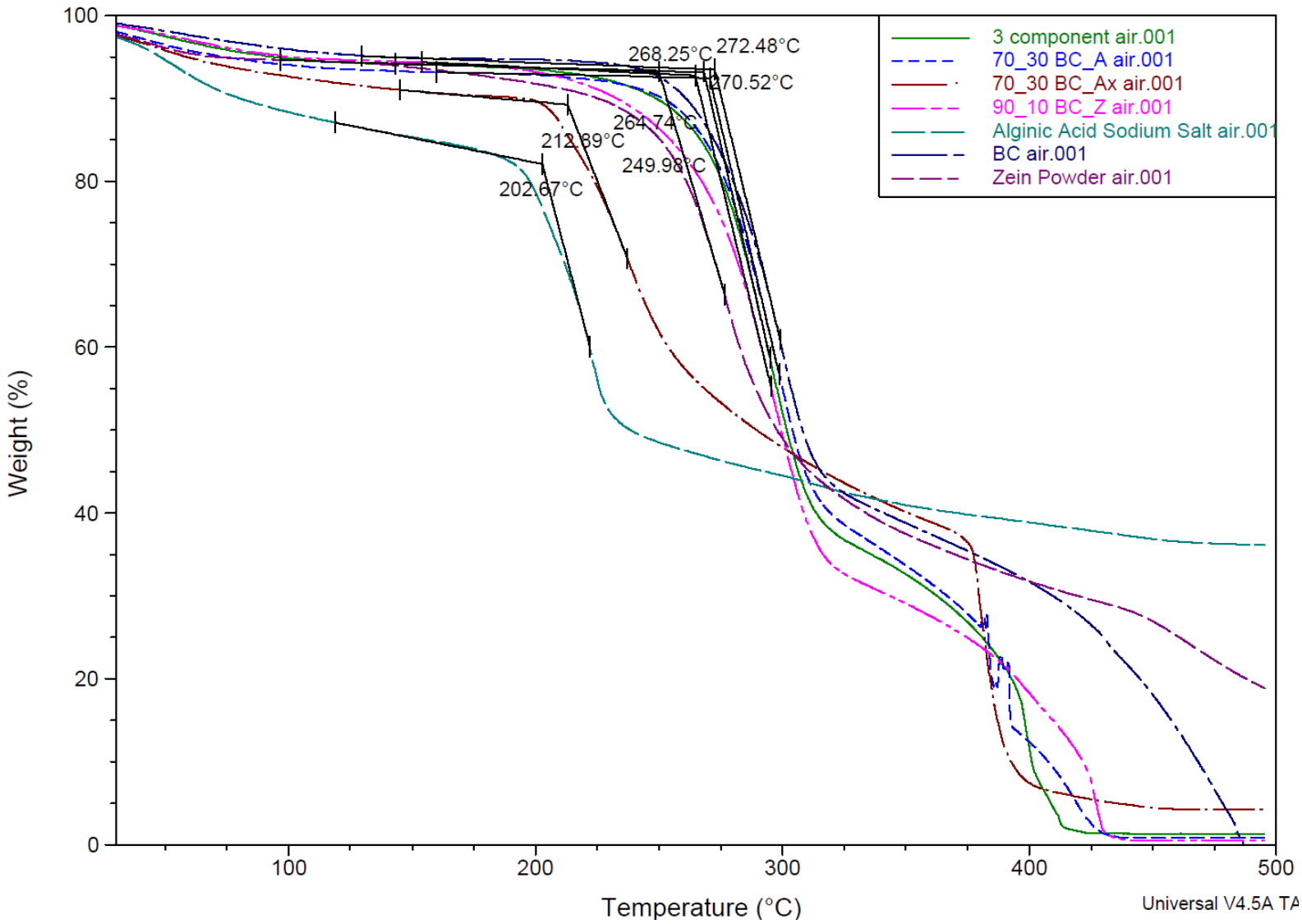

Figure A3. TG curve for vacuum filtered films in an air atmosphere

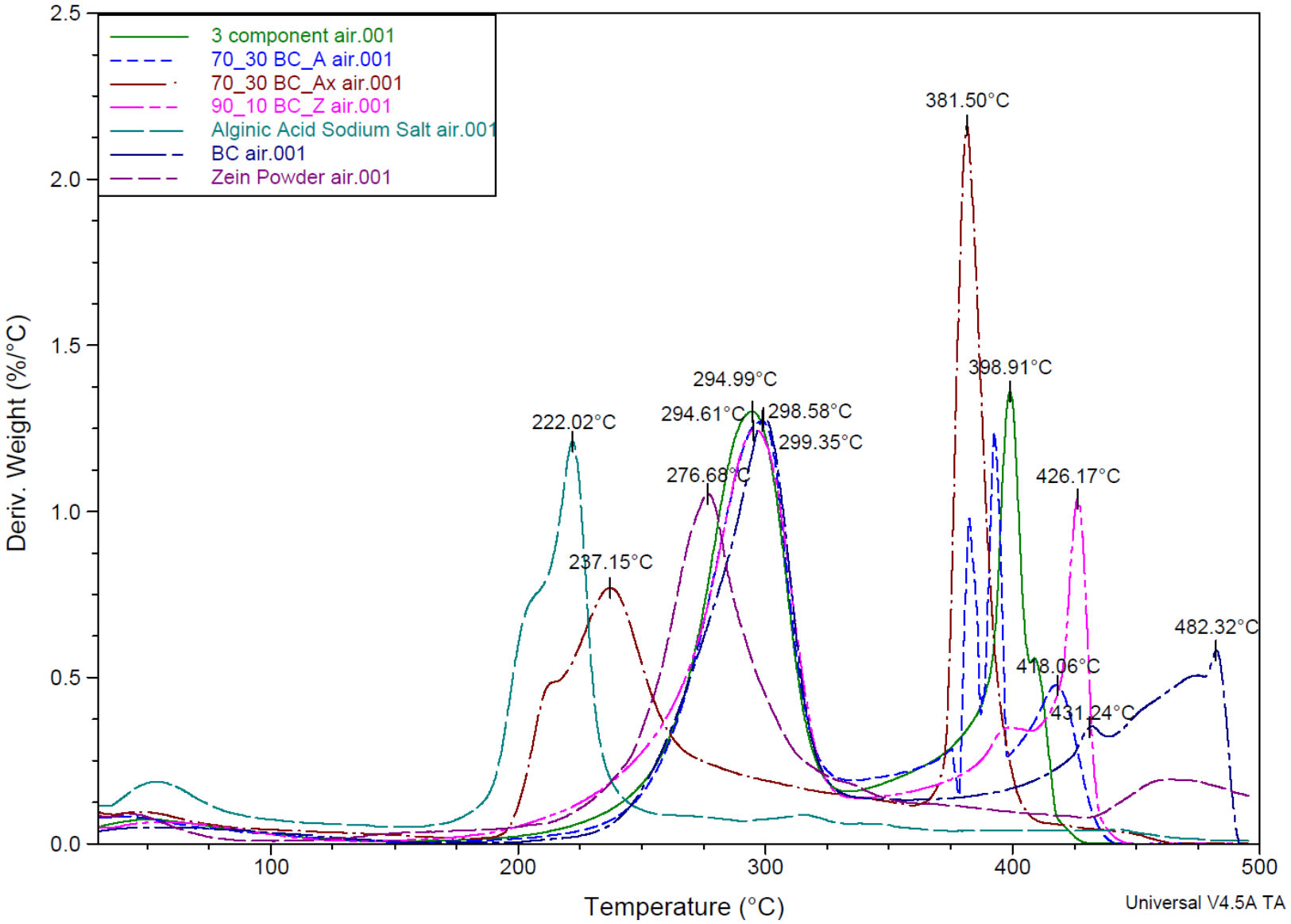

Figure A4. DTG curve for vacuum filtered films in an air atmosphere.

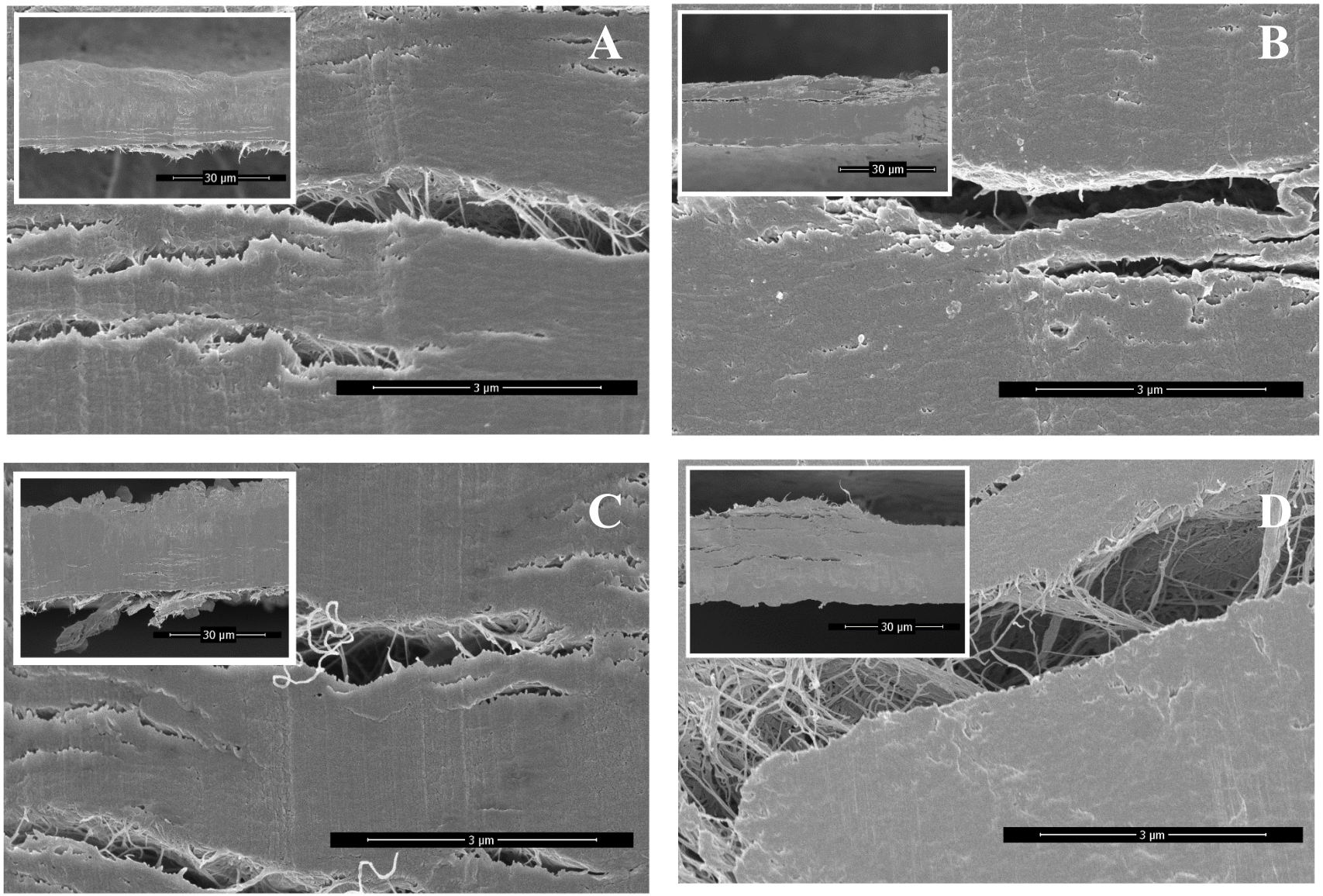

Figure A5. SEM micrographs of cast films at 1500x and 15000x magnification (A) 90:10 BC/Ax; (B) 80:10:10 BC/A/Zx; (C) 90:10 BC/Zx; (D) 80:10:10 BC/A/Z

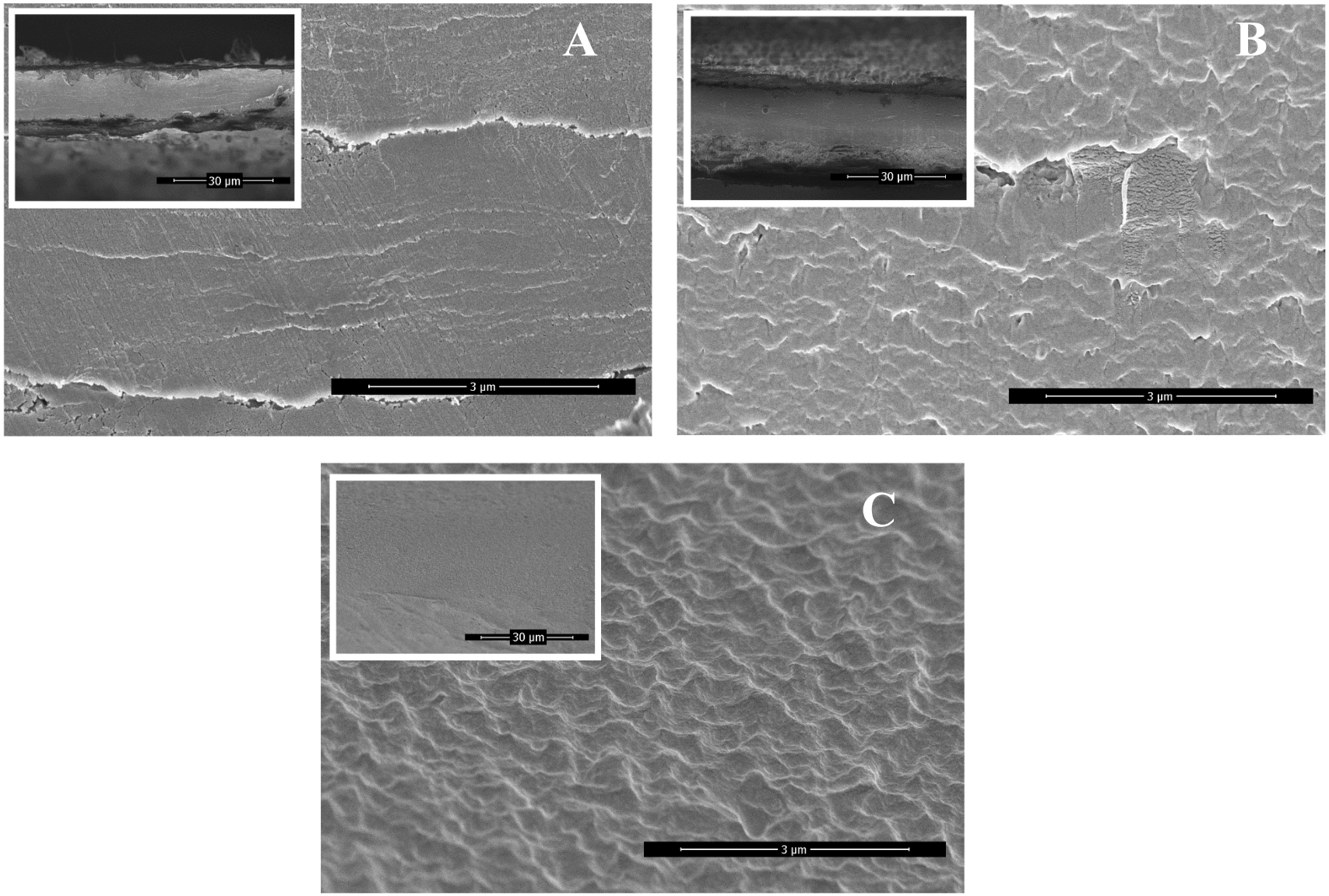

Figure A6. SEM micrographs of cast films at 1500x and 15000x magnification (A) neat BCx; (B) neat Zein x; (C) neat Alginate x

Appendix B – Supporting Information Chapter 3

Soy Lecithin Epoxidation

1:1.1 soy lecithin to formic acid:

25 g soy lecithin	62 g linoleic acid[125]	1 mol linoleic	2 mol C=C	1.1 mol formic acid	46.03 g formic
	100 g soy lecithin	200 g linoleic	1 mol linoleic	1 mol C=C	1 mol formic

= 7.84 g formic acid

1:1 formic acid to hydrogen peroxide:

7.84 g formic acid	1 mol formic acid	1 mol H_2O_2	37.01 g H_2O_2
	46.03 g formic acid	1 mol formic acid	1 mol H_2O_2

= 6.30 g H_2O_2

ESL and BCL Linkage

Determination of ESL content in reaction mixture:

25g soy lecithin + 7.84 g formic acid + 6.30 g H_2O_2 + 0.15 g PTSA = 39.29 g reaction mixture
(25 g soy lecithin / 39.29 g reaction mixture) * 100 = 63.6% Soy Lecithin

1:1.1 ESL/BCL assuming 100% conversion of epoxidation reaction:

10 g ESL mix	63.6 g ESL	1 mol ESL	2 mol epoxy	1.1 mol phenol on lignin	100 mol C9 on lignin[126]	1 mol lignin	6772 g lignin
	100 g ESL mix	462.51 g ESL	1 mol ESL	1 mol epoxy	66 mol phenol	39 mol C9	1 mol lignin

= 7.96 g lignin

Accounting for 2% ash content in lignin:

7.96 g lignin	100 g unwashed lignin
	98 g lignin

= 8.12 g unwashed lignin

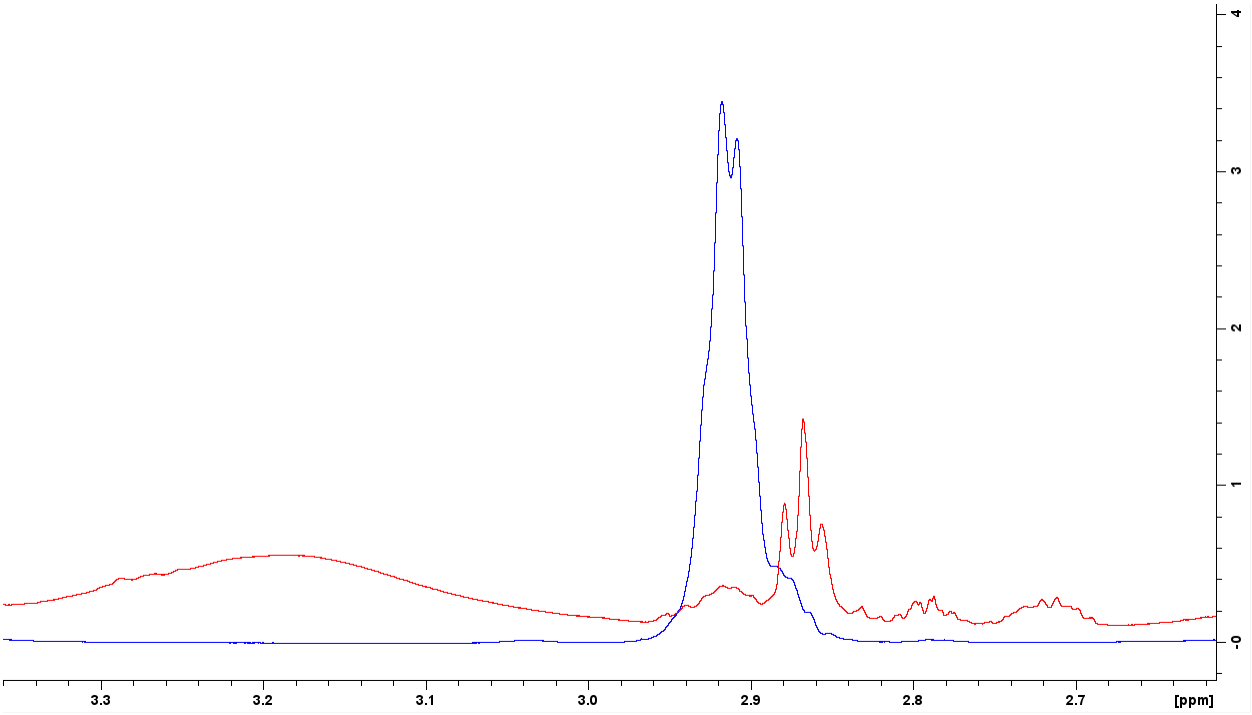

Figure B.1. 1D ^{1}H NMR Spectra of ESL and soy lecithin showing the ring-opening (~3.2 ppm) and epoxide hydrogens (~2.86 ppm)

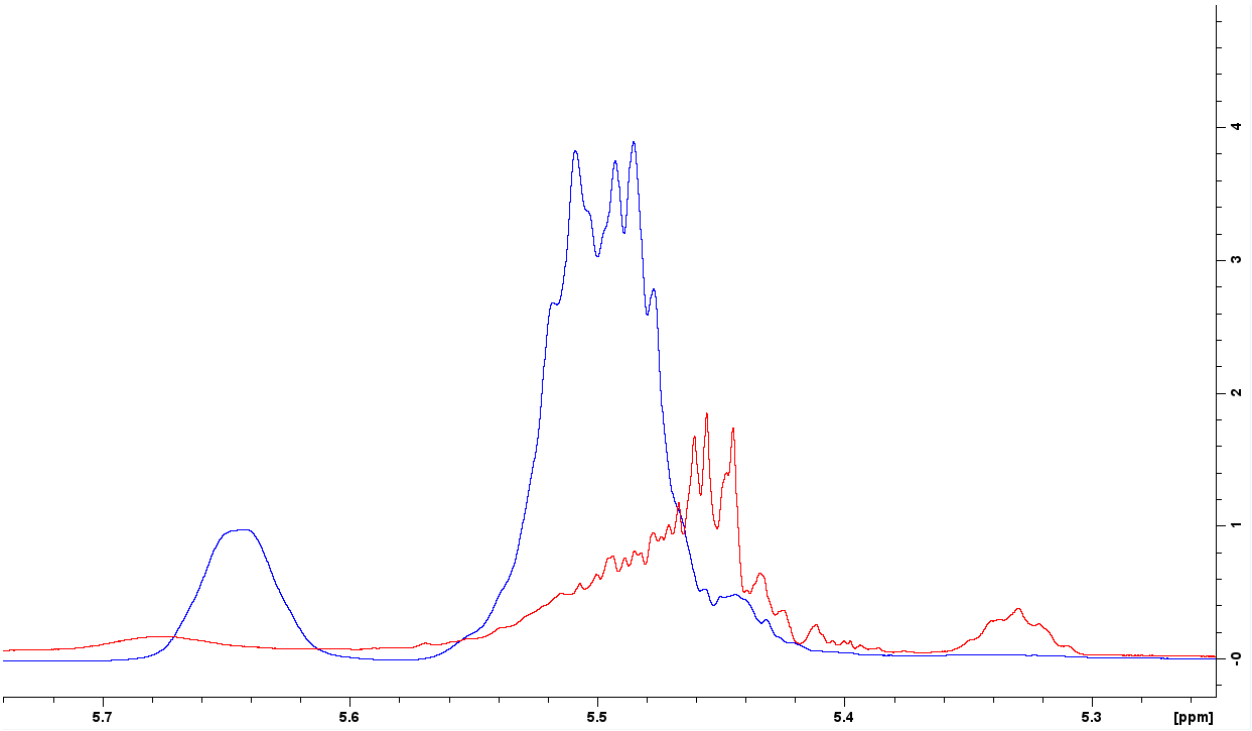

Figure B.2. 1D ^{1}H NMR Spectra of ESL and soy lecithin in d-toluene showing the reduction of vinylic hydrogens (~5.5 ppm).

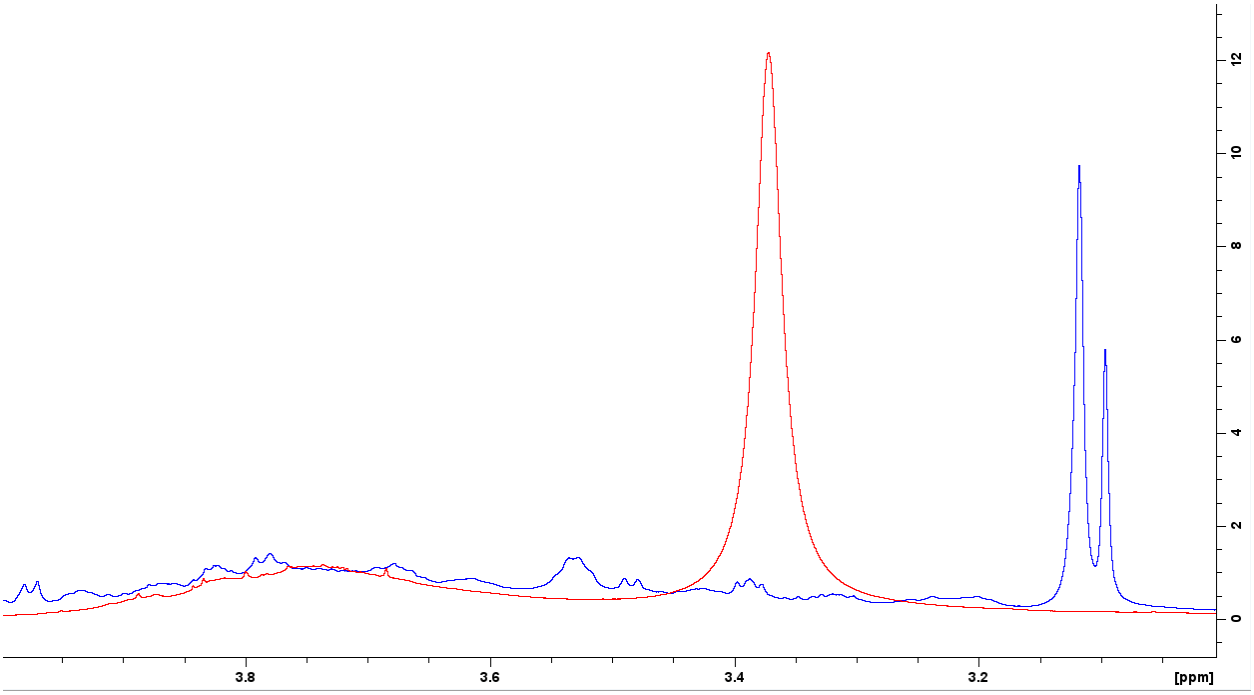

Figure B.3. 1D ^{1}H NMR spectra of ESL+L formulation and lignin in DMSO-d6 showing the aliphatic alcohol reduction (~3.4 ppm).

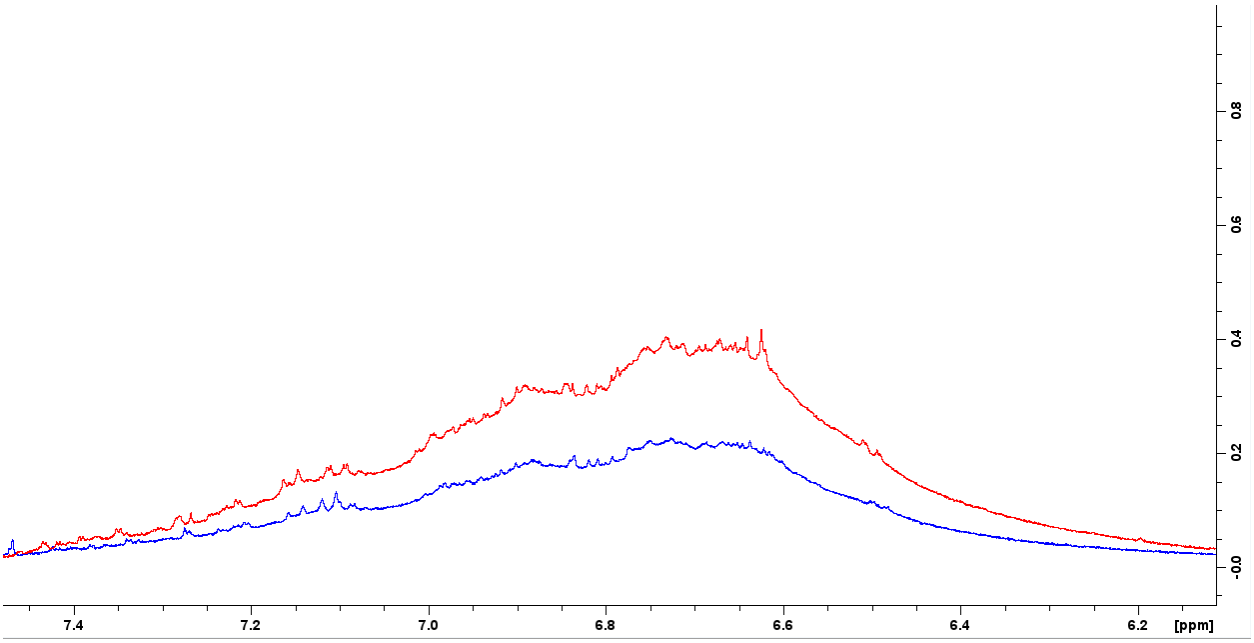

Figure B.4. 1D ^{1}H NMR spectra of ESL+L formulation and lignin in DMSO-d6 showing the phenolic alcohol reduction (~6.7 ppm).

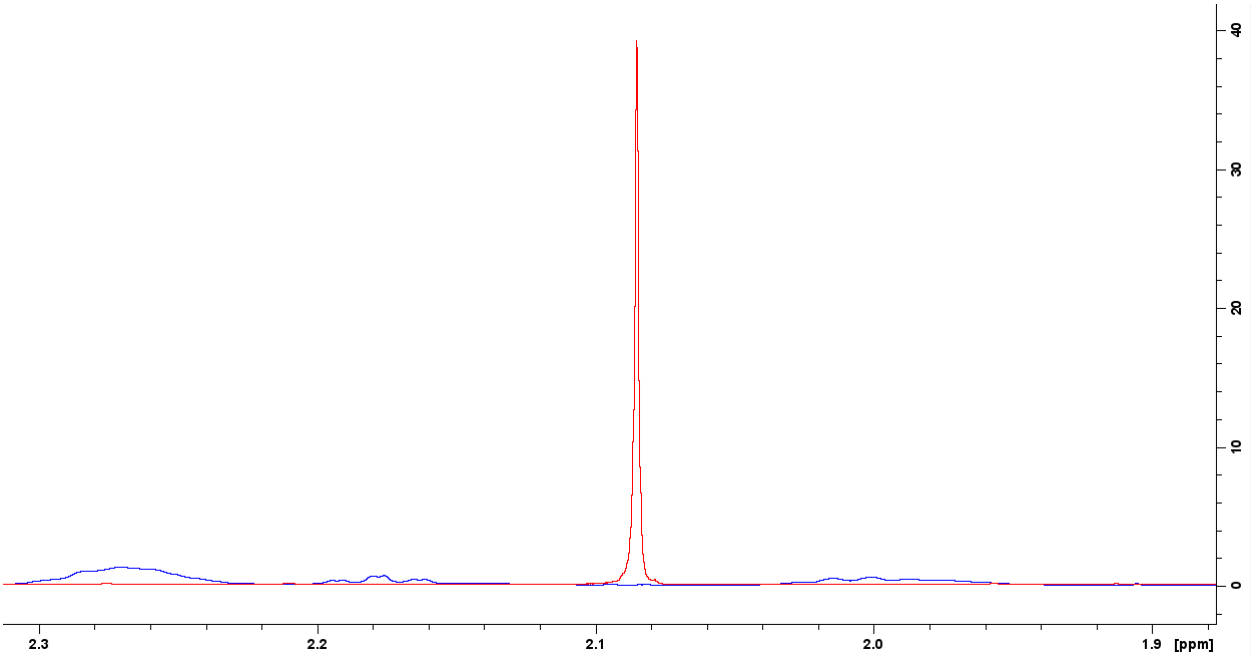

Figure B.5. 1D ^{1}H NMR spectra of ESL+L formulation and lignin in DMSO-d6 showing the disappearance of the thiol peak (~2.08 ppm).

Appendix C – List of Publications and Presentations

Poster Presentations

"A Bio-Based Alternative for Aseptic Packaging"

American Chemical Society Green Chemistry and Engineering Conference

Poster Session - Virtual, 2021

"Tensile Properties of Bacterial Cellulose Composite Films for Potential Applications in Aseptic Packaging"

NCSU College of Natural Resources Graduate Research Symposium

Poster Session - Virtual, 2021

Oral Presentations

"Tunable Barrier and Mechanical Properties of Bacterial Nanocellulose Composite Films"

American Chemical Society Spring Meeting

Oral Presentation - San Diego, CA, March 2022

Publications

Roman Sarder, **Emily V Piner**, David Cruz Rios, Lisandra Chacon, Mirela Angelita Artner, Nelson Barrios, and Demitris Argyropoulos. “Copolymers of starch , a sustainable template for biomedical applications: a review.” *Carbohydrate Polymers*, vol. 278, 2022, 118973

Martin A Hubbe, **Emily V Piner**, Nathalie Lavoine, and Lucian A Lucia. “Barrier Properties of Bionanocomposite Films.” in *Polymer Based Bio-nanocomposites - Properties, Durability and Applications*, edited by Chandrasekar Muthukumar et al. Springer Singapore, 2022

Appendix D – Awards and Service

Awards

First Place Poster

Master's Student – Forest Biomaterials

CNR Graduate Research Symposium – 2021

Goldstein Fellowship

Department of Forest Biomaterials

NC State University – 2022

Service

College of Natural Resources, Committee Member, Fall 2021

Review applications and select a nominee for college wide teaching awards.

Forest Biomaterials Analytical Team, Responsible User, 2020- present

Responsible for upkeep and maintenance of UV-Vis and TGA equipment. Responsible for training of new users for UV-Vis and TGA equipment.

Feed the Pack Food Pantry, Volunteer, Jan 2022 – present

Responsible for restocking and running the on campus food pantry